MASTER THESIS

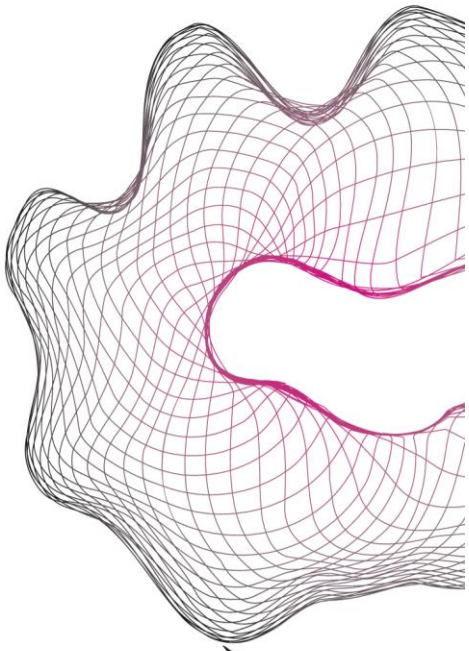

SOFT-TISSUE TUNING IN A PERSONALIZED MUSCULOSKELETAL KNEE MODEL USING QUANTITATIVE COMPARISON BETWEEN SIMULATED AND INTRAOPERATIVELY MEASURED KNEE LAXITY

Iris Matser

FACULTY OF ENGINEERING TECHNOLOGY
DEPARTMENT OF BIOMECHANICAL ENGINEERING

EXAMINATION COMMITTEE
Prof. Dr. Ir. N.J.J. Verdonschot
Dr. Ir. P. Tzanetis
Dr. Ir. R. Fluit

UNIVERSITY OF TWENTE.

5-7-2024

Soft-tissue tuning in a personalized musculoskeletal knee model using quantitative comparison between simulated and intraoperatively measured knee laxity

I. Matser

Abstract

Pre-operative planning of robotic assisted total knee arthroplasty (RA-TKA) is performed manually and may benefit from the use of a patient-specific musculoskeletal (MS) model. However, it is difficult to personalize the soft tissue properties in an MS model. In this study, the ability to personalize the reference strain of the ligaments in a previously developed knee-only MS model was evaluated. The model was personalized based on computed tomography (CT) scans, segmented to reconstruct the osteophyte-free state of the knee, of a single patient who underwent RA-TKA. Of this patient, intraoperative varus and valgus laxity tests were performed with the knee in full extension, and the resulting lateral and medial joint gaps were measured. A sensitivity analysis was then conducted to determine the sensitivity of the simulated joint gaps of the extended knee in the CT-based personalized model to changes in the ligament reference strains. Based on the resulting sensitivity, the ligament reference strains of the model were manually tuned in order to replicate the intraoperatively measured joint gaps. Nine tuning steps resulted in a simulated joint gap of 22.04 mm medially and 22.99 mm laterally. With a measured joint gap of 22 mm medially and 23 mm laterally, the differences between the simulated and measured joint gaps decreased from 1.50 mm to –0.04 mm medially and from 1.11 mm to 0.01 mm laterally. Although we used intraoperative measurements as a starting point to further personalize a MS model, as opposed to other studies, it was difficult to assess the accuracy of the resulting simulated joint gaps due to the lack of information on the intraoperatively applied force, model shifting, and high ligament strains. Furthermore, the tuning process was done manually and thus the optimal combination of reference strains could be different than found in this study. In summary, we were able to closely replicate intraoperatively measured joint gaps by manually tuning the soft tissue in a CT-based personalized MS model. An automated optimization process may contribute to a more optimal combination of reference strains to achieve similar results.

Keywords: Knee Laxity, Reference Strain, Ligament Tuning, Musculoskeletal Model, Total Knee Arthroplasty

1. Introduction

Total knee arthroplasty (TKA) is one of the most performed surgical procedures in patients with advanced knee osteoarthritis (OA). However, up to 20% of the patients undergoing conventional TKA remain dissatisfied with the outcome of the procedure [1] [2]. Over the past decades, robotic assisted TKA (RA-TKA) systems have been introduced to improve clinical outcome. [3] Studies show improved component positioning accuracy and precision compared to conventional TKA [3] [4] [5] [6], leading to lower revision rates and lower risk of systemic complications [7].

An example of a RA-TKA system is the Mako system (Stryker, Kalamazoo, Michigan, USA), which is used for both the surgical procedure and creating a surgical bone resection and implant positioning plan. The initial surgical plan is created manually and is established using mechanical alignment (MA) based on the pre-operative computed tomography (CT) data of the patient, resulting in a neutrally aligned knee. [8] [9] However, research has shown that a large fraction of the normal population has constitutional varus alignment of the knees. [10] Therefore, MA may not be the optimal solution for all patients undergoing RA-TKA. In order to change the MA based pre-operative plan, the surgeon can pre-operatively modify this surgical plan using the Mako software based on the joint lines of the patient as determined with a pre-operative X-ray and the planned position of the implant, creating a kinematically aligned knee [9]. Additionally, the surgeon can use functional alignment (FA) to intraoperatively adapt the plan based on soft-tissue balancing, determining the laxity of the knee when applying a varus or valgus force. [9] [11] Using FA, the medial and lateral joint gaps are balanced, which leads to a surgical plan resulting in a medial resection gap of 18-19 mm in extension and flexion with an added lateral laxity of 1-2 mm. [11] However, the target for optimal component positioning remains unclear. To make the implant position planning more precise and patient-specific, and to recreate the functional aspects of the knee before OA, regenerating the pre-diseased knee function may be more eligible. [12]

While the implant positioning with the Mako system is highly accurate [13] [14], the pre-operative planning procedure is manual and thus operator-dependent. The use of a musculoskeletal (MS) knee

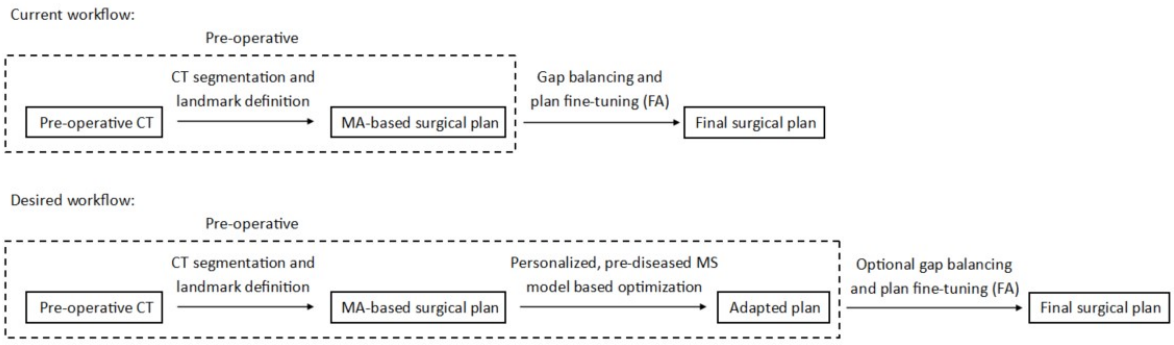

Figure 1: Current workflow of the planning phase of RA-TKA (top) and desired workflow including MS model based optimization (bottom)

model that simulates the osteophyte-free knee, and thus from a geometrical point of view imitates the pre-diseased state, could be of added value for precise patient-specific implant position planning and joint gap balancing during the pre-operative phase, as can be seen in Figure 1. This creates a more automated workflow and more patient-specific surgical plan, resulting in more accurate implant positioning. However, a considerable limitation of MS models is the difficulty of personalizing soft tissue, due to the lack of subject-specific mechanical properties, such as the reference strain and stiffness of ligaments. These soft tissue properties are usually an assumption based on literature, and therefore not patient-specific. [12] [15] [16] [17] It is challenging to include personalized soft tissue properties to an MS model: determining ligament properties cannot be done with CT-data alone and thus requires additional imaging modalities [18] [19], methods to directly measure mechanical ligament properties such as stiffness and reference strain are often invasive [18] or studied on cadaveric knees [19] [20] [21], and noninvasive in-vivo techniques are mostly based on estimations [20] [22]. Furthermore, a personalized model's behavior should be compared with intraoperative measurements in order to validate the accuracy of the model. [12] [16] [17]

Therefore, a starting point for eventually being able to add ligament properties in a personalized MS model, would be to compare the knee joint laxity of the MS model with intraoperative laxity measurements. The intraoperative measures acquired during this study are the lateral and medial joint gaps during varus and valgus stress tests, hereafter referred to as laxity tests, obtained by the Mako system during the joint balancing phase [9]. The joint gaps resulting from the modeled laxity tests may be used to assess the model's sensitivity to changes in the ligament properties by analyzing the change in the modeled knee joint gaps in response to ligament property changes. The resulting sensitivity could be subsequently used for tuning the model's ligament properties to replicate the intraoperative joint gap measurements with the model, thereby resulting in an estimation of the patient-specific ligament mechanics. This may provide insights into the possibility of personalizing the soft tissue of the MS model. [12]

While an actual optimization process is beyond the scope of this study, a sensitivity analysis and tuning of the soft-tissue properties of the model could give insight into the ability of the model to replicate intraoperatively measured data. Therefore, the research question was: to what extent can the soft tissue in a CT-based personalized MS model be tuned to minimize the difference between simulated joint gaps and the corresponding intraoperatively measured joint gaps? This research question can be divided into three aims. The first aim is to perform intraoperative knee laxity measurements on one patient undergoing RA-TKA with the Mako system. The second aim is to determine the sensitivity of the lateral and medial knee joint gaps in a previously developed CT-based patient-specific MS knee model [23] to changes in the reference strain of the individual knee ligament bundles. The third aim is to tune the ligament's mechanical properties in the model in order to evaluate whether the model can simulate the intraoperatively measured joint gaps. Based on the findings in this study we assess whether the personalized model could be utilized in the pre-planning for RA-TKA procedures in the future.

2. Methods

An overview in the form of a workflow of the steps described below can be found in Figure 2.

2.1. Patient data collection

To achieve the first aim of this study, pre- and intraoperative data were collected at Policlinico di Modena in Italy [1]. The data consisted of pre-operative CT scans of the by knee OA affected leg, the planned MA-based femoral and tibial bone resections, and intraoperative knee laxity measurements of one patient who underwent RA-TKA. The planned bone resections were ob-

[1] Patients at Policlinico di Modena sign privacy papers prior to the surgery in which they give permission that their data may be used for scientific research purposes

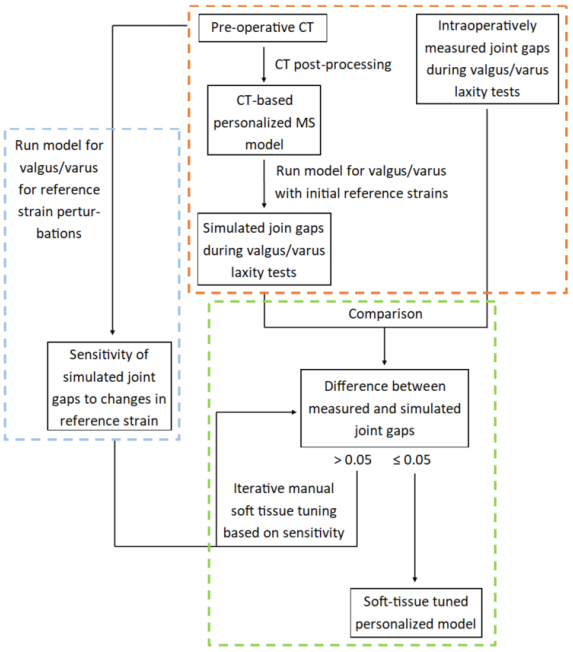

Figure 2: Workflow of the steps described in methods: patient data collection (orange), the sensitivity analysis (blue) and tuning the model (green), where the workflow starts at the top and ends at the bottom

tained using the Mako system. [24] The intraoperative measurements were obtained according to the measurement protocol, provided in Supplement 1. This resulted in a database of pre- and post-implant laxity measurements, consisting of medial and lateral knee joint gaps for 0° and 90° flexion, for three situations, hereafter referred to as laxity tests. For the laxity tests, the surgeon first placed a surgical spacer spoon between the distal femoral condyle and the proximal tibial condyle on the least affected side of the knee, according to the surgical protocol [8]. In the case of the patient selected for the data collection of the present study, who had a varus knee and thus more bone wear on the medial side of the knee, the spacer spoon was placed on the lateral side. The surgeon then applied tension to the spoon, opening up the joint gap on that side, and proceeded with the laxity tests. The no-stress laxity test is the neutral situation, in which no varus or valgus stress was applied on the knee joint in addition to the spacer spoon tension. For the valgus laxity test, a valgus stress was applied to the knee, opening up the medial joint gap. The no-stress and valgus laxity tests are part of the surgical protocol for a patient with a varus knee. For this study, a varus laxity test was added, in which a varus stress was applied to the knee, opening up the lateral joint gap. During all laxity tests, the medial and lateral joint gaps were recorded from the screen of the Mako system. A more detailed explanation of the workflow of the surgery, including the laxity measurements, can be found in Supplement 2. Because of unforeseen limited time during this study, only the pre-implant laxity tests in 0° flexion were used.

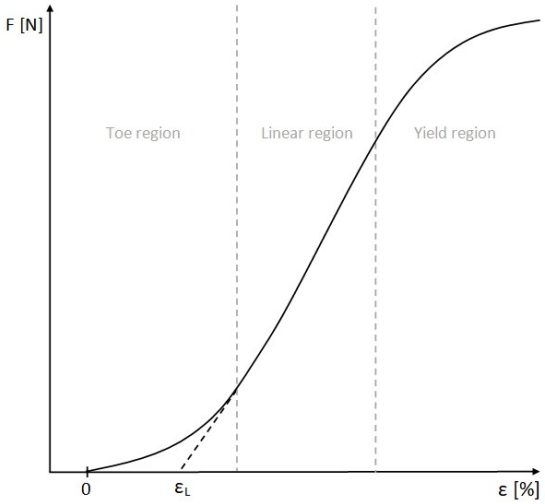

Figure 3: Non-linear force-strain relationship of the ligaments in the MS model

2.2. The musculoskeletal model

The musculoskeletal model used for this study is a previously developed knee MS model that consists of a fixed distal femur, a proximal tibia and a patella, and the corresponding muscles and ligaments [23]. The ligaments are modeled based on a non-linear force-strain relationship [23], which is visualized in Figure 3 and can be described by:

$$\begin{aligned} F &= \frac{1}{4}\, k \frac{\varepsilon^2}{\varepsilon_L}, && 0 \le \varepsilon \le 2\varepsilon_L \\ F &= k(\varepsilon - \varepsilon_L), && \varepsilon > 2\varepsilon_L \\ F &= 0, && \varepsilon \le 0 \end{aligned} \tag{1}$$

where F is the force, k is the stiffness of the ligament, ε is the strain of the ligament, and ε_L is the non-linear strain level parameter [25] [26], which is set to 0.03 in the used MS model. The strain ε can be described by

$$\varepsilon = \frac{L - L_0}{L_0} \tag{2}$$

where L_0 is the zero-load or slack length. [25] [26] The slack length can in turn be described by

$$L_0 = \frac{L_R}{\varepsilon_R + 1} \tag{3}$$

where L_R is the reference length of the ligament, and ε_R is its reference strain. [25] [26] The ligament properties of the model are thus defined by the stiffness k and reference strain ε_R. As a previous study with a similar MS model showed that their model was more sensitive to changes in reference strain than stiffness [27], only the ligament reference strain were considered in this study. The ligament reference strains in the used MS model are mostly originally adapted from literature, with a few exceptions where the reference

strain was adjusted to the model. [23] An overview of these initial reference strains of each ligament bundle can be found in Table 1.

Table 1: Initial model reference strains and perturbations

Ligament bundle	ε_R - 0.1	Initial ε_R [%]	$\varepsilon_R + 0.1$
aACL	0.25	0.35	0.45
pACL	0.25	0.35	0.45
aPCL	-0.56	-0.46	-0.36
pPCL	-0.13	-0.03	0.07
OPL	0	0.1	0.2
PC	-0.03	0.07	0.17
a_dMCL	-0.27	- 0.17	- 0.07
m_dMCL	-0.16	-0.06	0.04
p_dMCL	-0.16	-0.06	0.04
a_sMCL	-0.09	0.01	0.11
m_sMCL	-0.09	0.01	0.11
p_sMCL	-0.09	0.01	0.11
aLCL	-0.09	0.01	0.11
mLCL	-0.09	0.01	0.11
pLCL	-0.09	0.01	0.11
aALL	-0.07	0.03	0.13
pALL	-0.07	0.03	0.13

The MS model was personalized using CT-data of the research subject, which was segmented to obtain the subject specific bony geometry for visualization and simulation purposes, and, subsequently, post-processed to obtain bony landmarks to scale the MS model to the anatomy of the research subject. A more detailed description of the postprocessing workflow of the CT data, including segmentation, can be found in Supplement 3.

2.2.1. Model adaptations

In order to replicate the intraoperative measurements as accurately as possible, four major aspects of the MS model were adapted. The first adaptation was the selection of the included ligaments. The original MS model included twelve ligaments, including patellar ligaments. As the intraoperative measurements were done without involvement of the patella, the ligaments included in the MS model are the remaining ligaments of the original model: the anterior cruciate ligament (ACL), posterior cruciate ligament (PCL), oblique popliteal ligament (OPL), posterior capsule (PC), deep and superficial medial collateral ligament (dMCL/sMCL), lateral collateral ligament (LCL), and anterolateral ligament (ALL), as shown in Figure 4. These ligaments, except for the OPL, consist of multiple bundles.

The second adaptation was the location of the force application node and the direction of the applied force for the varus and valgus laxity tests. In the original MS model, the force application node was defined in the anatomical frame of the tibia and the force was applied laterally or medially. To more accurately match the way a varus or valgus force was applied during the intraoperative measurements, the force application node was moved to the lateral and medial tibial condyle for the varus and valgus laxity tests, respectively. The force itself was changed to a distally directed force, to move the tibia away from the femur distally and create a medial or lateral joint gap. The force was set to 50 N (Appendix A).

The third adaptation was the definition of the joint gap. In the original MS model, the joint gap was defined as the distance between the anatomical frames of the femur and the tibia. To match the joint gap defined by the Mako system, the joint gap in the model was redefined as the distance between the resected bones of the medial femoral epicondyle and the medial tibial condyle, and between the resected bones of the lateral femoral epicondyle and the lateral tibial condyle, for the medial and lateral joint gaps, respectively. A more detailed description of how the joint gaps were redefined can be found in Appendix B.

The fourth adaptation was the addition of an offset to the tibial contact surface, in order to simulate the aforementioned spacer spoons used intraoperatively to open up the joint gap on the least affected side of the knee. As adding an extra surgical instrument in the model to recreate the intraoperatively used spacer spoon would have been more complicated than using what was already present in the model, i.e. the tibial contact surface, the latter option was chosen. The needed tibial offset was calculated using the initial lateral joint gap when a no-stress test was run with the model, and the intraoperatively measured corresponding joint gap, using:

$$Y_{\mathrm{TOS}} = JG_{\mathrm{meas}} - JG_{\mathrm{model}}$$

where Y_{TOS} is the tibial offset, JG_{meas} is the joint gap as measured intraoperatively in the neutral situation in full extension, and JG_{model} is the initial joint gap resulting from running the personalized model for the no stress situation, in which the model finds an equilibrium and then stops. The tibial offset was calculated as a translation in the y-direction. In this case, the intraoperatively measured lateral joint gap was 22 mm, and the simulated lateral joint gap by running the no stress test in the model was 16.44 mm. Therefore, the needed lateral tibial offset was 22 - 16.44 = 5.56 mm.

2.3. The sensitivity analysis

As the second aim of this study was to evaluate the sensitivity of the lateral and medial knee joint gaps to changes in the reference strain of the individual ligament bundles of the ACL, PCL, OPL, PC, dMCL, sMCL, LCL and ALL in the personalized MS model, a sensitivity study was conducted. This was done by running the model for valgus and varus laxity tests,

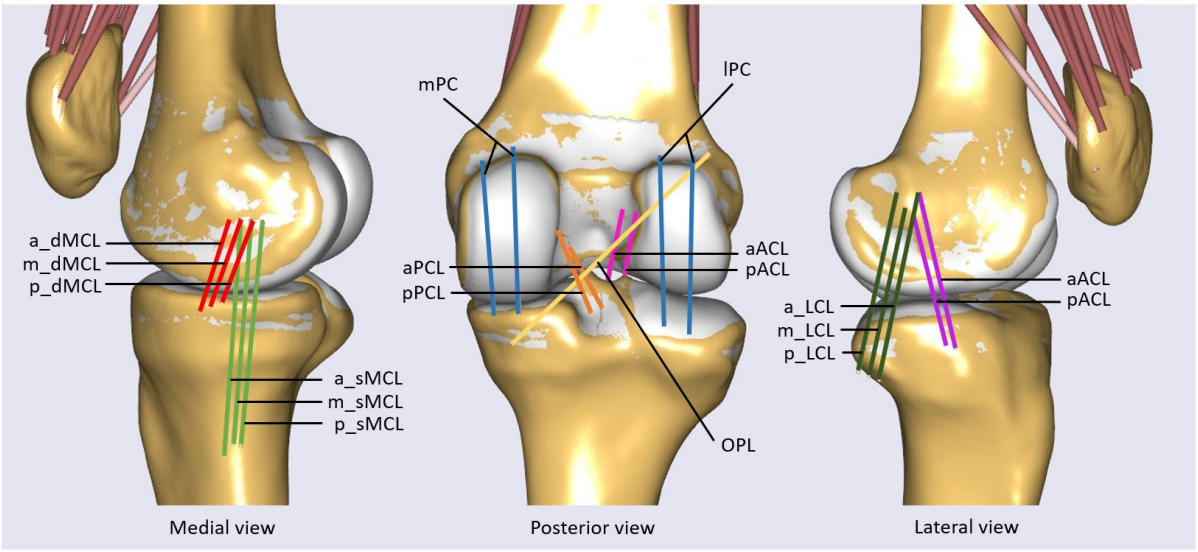

Figure 4: The included ligaments as modeled in the CT-based personalized MS model (right knee) in AnyBody: the anteromedial and posterolateral anterior cruciate ligament (aACL/pACL); the anterolateral and posteromedial posterior cruciate ligament (aPCL/pPCL); the oblique popliteal ligament (OPL); the posterior capsule (PC); the anterior, middle and posterior deep medial collateral ligament (a_dMCL/m_dMCL/p_dMCL); the anterior, middle and posterior superficial medial collateral ligament (a_sMCL/m_sMCL/p_sMCL); the anterior, middle and posterior lateral collateral ligament (aLCL/mLCL/pLCL); the anterior and posterior anterolateral ligament (aALL/pALL)

in 0° flexion, for perturbations of ± 0.1 of the reference strain of all the ligament bundles, using a custom algorithm provided in Appendix C. It is important to note that when the reference strain of one ligament bundle was changed, the reference strains of the other ligament bundles remained the same. Table 1 shows the reference strain values for all perturbations. For each perturbation, the lateral and medial joint gaps were obtained, as well as the strains in all the ligament bundles. The resulting joint gap values of running the model for the initial reference strain values as noted in Table 1 were compared to the intraoperatively measured joint gap values by calculating the difference. The resulting joint gap values of the ± 0.1 [%] perturbations were used to determine the difference with the initial joint gap values, creating an overview of the sensitivity of the model's joint gaps to changes in the reference strains of the ligament bundles.

2.4. Tuning the model

As the third aim of this study was to tune the soft-tissue properties of the model to evaluate its ability to simulate intraoperatively measured joint gaps, the results of the sensitivity study were used to manually tune the reference strains of the ligament bundles. This was done step-by-step, tuning the ligament bundles with the largest effect on the joint gap first. For each reference strain adaptation, the resulting modeled joint gaps were then again compared to the intraoperatively measured joint gaps to determine whether more tuning was needed.

3. Results

3.1. Patient data collection

Table 2 shows the intraoperatively measured lateral and medial joint gaps of the pre-implant situation, for 0° and 90° flexion, for the neutral situation as well as the varus and valgus laxity tests. A more extensive database can be found in Appendix D. Table 2 shows that during the intraoperative measurements for the no stress situation, the joint gaps for 0° flexion were 22 mm and 20 mm for the lateral and medial side, respectively. When applying varus stress, the varus angle increased from 3 ° to 9 ° , and the lateral and medial joint gap changed to 23 mm and 17 mm, respectively. As the varus laxity test was used to determine the lateral laxity of the knee, we can conclude that the lateral laxity of this patient's knee was 23 mm - 22 mm = 1 mm. The same calculation can be done for the medial side, using the measured values during the valgus laxity test, resulting in a medial laxity of 22 mm - 20 mm = 2 mm.

Table 2: Intraoperatively measured joint gaps

Laxity test	Flexion degree	Intraoperatively measured values		
		Varus/valgus angle [°]	Lateral joint gap [mm]	Medial joint gap [mm]
No stress	0°	3	22	20
	90°	1	18	18
Varus	0°	9	23	17
	90°	3	20	-*
Valgus	0°	2	21	22
	90°	3	-*	19

*For 90° flexion, the lateral and medial joint gaps were measured simultaneously

Only the measured values in 0° flexion were used for the sensitivity analysis and the tuning process. Therefore, the Mako screen recordings for the intraoperative measurements during the valgus and varus laxity tests in 0° flexion are shown in Figure 5. As the laxity tests were done during the ligament balancing phase, Figure 5 contains screenshots of the ligament balancing page.

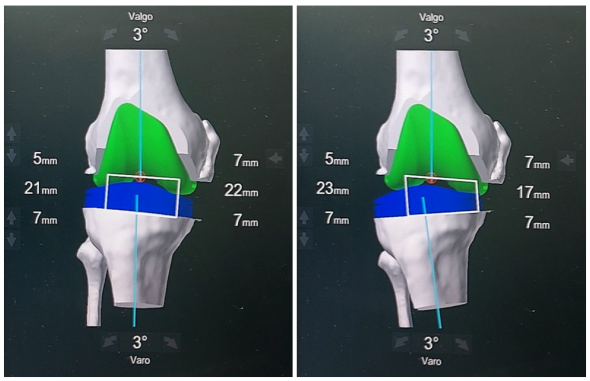

Figure 5: Screenshots of the Mako screen recordings during the intraoperative valgus (left) and varus (right) laxity tests in 0° flexion

3.2. The sensitivity analysis

The results of the sensitivity analysis are shown in Figure 6. The bar chart show the change in lateral and medial joint gaps with respect to the initial joint gaps (red line) in the model for changes in the reference strain for each ligament bundle, as a result of the sensitivity analysis where the reference strains were perturbed with ± 0.1 [%]. The intraoperatively measured joint gaps are also shown (green line) to give an indication of how the simulated joint gaps change with respect to the measured values for each reference strain perturbation. An overview of the results of the sensitivity analysis, including the changes in the strains of each ligament bundle, is shown in Appendix E.

3.3. Tuning the model

Figure 7 shows the result of the tuning process for 0° flexion, where the difference between the simulated and intraoperatively measured medial and lateral joint gaps were calculated for each tuning step. 'Tuning step' 0 represents the model with the initial reference strain settings. The tuning steps and the corresponding reference strain adaptations are shown in Table 3. A more detailed explanation of the tuning steps can be found in Appendix F.

The final deviation of the simulated joint gaps from the intraoperatively measured joint gaps for the valgus and varus laxity tests, of the personalized model with its initial reference strain settings, and the personalized model after tuning the reference strains, is

Table 3: Tuning steps and the corresponding ε_R adaptations

Tuning step	Tuned ligament	Tuned bundle	ε_R adaptation
1	sMCL	all	-0.1
2	dMCL	all	-0.05
3	LCL	all	-0.08
4	PC	medial & middle-medial	-0.1
5	PC	medial & middle-medial	+0.05
6	sMCL	all	-0.05
7	OPL	-	-0.1
8	PC	middle-lateral & lateral	-0.1
9	ACL	posterior	-0.06

shown in Figure 8. For the initial reference strain settings, the simulated medial gap for the valgus laxity test was 20.50 mm. As the measured medial joint gap was 22 mm, the difference between the simulated and measured joint gap was 1.50 mm. The difference between the simulated and measured lateral joint gap for the varus laxity test was 1.11 mm, given that the simulated joint gap was 21.89 mm as opposed to the measured joint gap of 23 mm. After tuning the reference strains, the simulated medial joint gap for the valgus laxity test was 22.04 mm, and the simulated lateral joint gap for the varus laxity test was 22.99 mm. This resulted in a smaller difference between the simulated and measured joint gaps: -0.04 mm medially for the valgus laxity test, which is a 0.18% difference from the measured value, and 0.01 mm laterally for the varus laxity test, which is a 0.04% difference from the measured value. The negative difference implicates that the simulated joint gap was bigger than the measured joint gap. The effect of each tuning step on the joint gaps and ligament strains during the valgus and varus stress tests can be found in Appendix G.

To visualize the effects of the tuning process in addition to the quantitative difference between the simulated and measured joint gaps, the medial joint gap for a modeled valgus laxity test is shown in Figure 9 as an example, where the modeled medial joint gap is visualized for the model with the initial ligament reference strains, as well as the model with the ligament reference strains after the nine tuning steps described in Table 3.

4. Discussion

4.1. Interpretation of the results

This study investigated the extent to which the soft tissue in a CT-based personalized MS model could be tuned in order for the difference between simulated joint gaps and the corresponding intraoperatively measured joint gaps to be minimized. To achieve this, intraoperative knee laxity measurements on a single patient undergoing RA-TKA were performed, a sensitivity analysis to determine the sensitivity of the joint

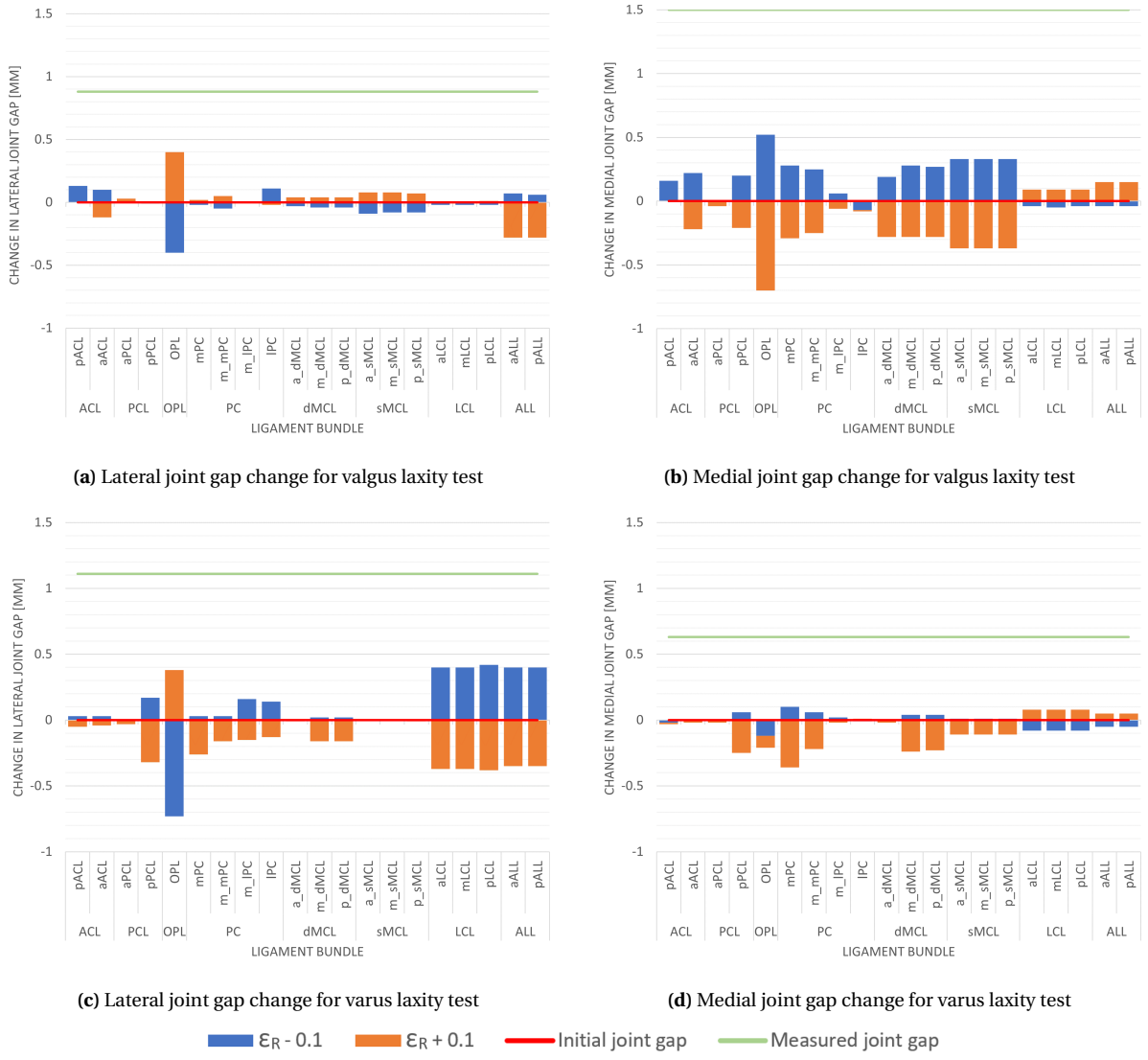

(a) Lateral joint gap change for valgus laxity test

(b) Medial joint gap change for valgus laxity test

(c) Lateral joint gap change for varus laxity test

(d) Medial joint gap change for varus laxity test

Figure 6: Change in lateral (left) and medial (right) joint gaps with respect to the initial joint gaps for changes in reference strain per ligament bundle for valgus (a and b) and varus (c and d) laxity test for the following ligaments: the anteromedial and posterolateral anterior cruciate ligament (aACL/pACL); the anterolateral and posteromedial posterior cruciate ligament (aPCL/pPCL); the oblique popliteal ligament (OPL); the posterior capsule (PC); the anterior, middle and posterior deep medial collateral ligament (a_dMCL/m_dMCL/p_dMCL); the anterior, middle and posterior superficial medial collateral ligament (a_sMCL/m_sMCL/p_sMCL); the anterior, middle and posterior lateral collateral ligament (aLCL/mLCL/pLCL); the anterior and posterior anterolateral ligament (aALL/pALL)

gaps in the model to changes in ligament reference strains was conducted, and the ligament reference strains in the model to minimize the difference between the simulated and measured joint gaps were tuned. The findings of this study show that tuning the ligament reference strains of a CT-based personalized MS model can minimize the difference between the simulated and intraoperatively measured joint gaps, suggesting that the model could be usable in the preplanning phase of RA-TKA procedures.

The difference between the intraoperatively measured and simulated joint gap of 1.50 mm medially and 1.11 mm laterally might appear insignificant. However, research by Tzanetis et al. [23] shows that a proximal-distal translation of 0.8 mm, caused by severe osteophytes, leads to increased an ligament strain of the ACL well above its damage threshold, which is clinically relevant according to Butler et al. [28]. It can thus be confidently stated that gap differences of 1.50 mm and 1.11 mm are clinically relevant and should therefore be reduced by ligament tuning.

The intraoperatively measured joint gap was larger than the initial joint gap of the MS model on the lateral as well as the medial side (Figure 6). This means that the modeled knee should be more lax on both the lateral and the medial side. Of the resulting changes in simulated joint gaps for the varus and valgus laxity tests (Figure 6), the measured medial joint gap for the valgus laxity test (Figure 6b), and the measured lateral joint gap for the varus laxity test (Figure 6c),

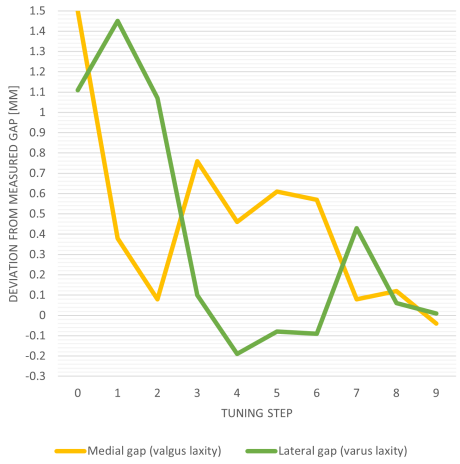

Figure 7: Deviation of simulated versus measured joint gap for each tuning step

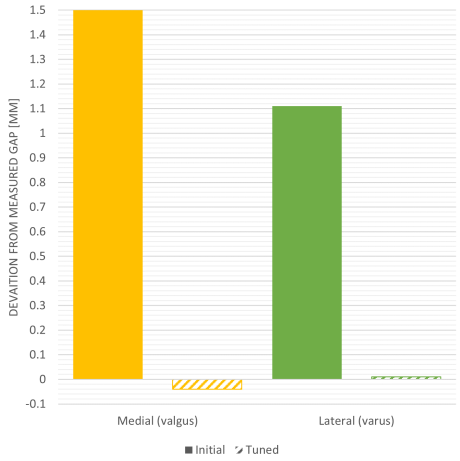

Figure 8: Deviation of simulated versus measured joint gap (initial versus tuned soft-tissue settings)

are most important when tuning the personalized MS model, as these values can give an indication of how close the modeled laxity is to the measured laxity. For the valgus laxity test, the medial joint gap was more sensitive to changes in the reference strains in general, and for the varus laxity test, the lateral joint gap was more sensitive to changes in the reference strains. This might be explained by the fact that during a valgus stress, the medial ligaments are tensioned, and during a varus stress, the lateral ligaments are tensioned. More specifically, for the valgus laxity tests, the reference strains in the dMCL and sMCL, and the two medial bundles of the PC had a large effect on the medial joint gap, as can be seen in Figure 6b. This aligns with the findings of Robinson et al. [29], who found that the sMCL is the primary restraint to valgus movement of the knee, the dMCL is the secondary restraint, and the medial PC resists 32% of valgus movement of the knee. Studies by Seering et al. [30] and Swinford et al. [31] also confirm these findings. Moreover, Figure 6b shows that the aACL and the pPCL had a large effect on the medial joint gap. Research by Miyasaka et al. [32] shows that when a varus force was applied in extension, the strain in the ACL increased significantly, and when a varus force was applied in flexion, the strain in the PCL increased. The same happened when applying a valgus force, but to a smaller extent. They also state that the ACL has a higher strain in extension, as opposed to the PCL, which has a higher strain in flexion. [32] Based on these findings, we would expect mainly the ACL to have an effect on the joint gaps, as all simulations were done for full extension only. However, our findings did not confirm this hypothesis: Figure 6 shows that changes in the reference strain of both the ACL and PCL affected the joint gaps. This is in accordance with other studies that show that the ACL, besides restraining anterior translation, also resists valgus loads in the knee [33] [34], and that the PCL has a secondary restraining role during varus and valgus movement [20]. For the varus laxity tests, the LCL, ALL and the lateral bundles of the PC seem to have had the largest effect on the lateral joint gap, as can be seen in Figure 6c. This is in accordance to research by Seering et al. [30], which shows that the ALL carries 72% of the applied load during a varus laxity test, and research by Wilson et al. [20], which shows that the LCL provides the primary restraint during a varus movement. Another important observation is the effect of the OPL on the joint gaps. As shown in Figure 6, the OPL had a large effect on both the medial and lateral joint gap, for the varus as well as the valgus laxity tests. Given the fact that the OPL mainly prevents hyperextension of the knee [35] [36], it will be stretched during full extension. It is therefore possible that the OPL plays an important role in the laxity when the knee is fully extended. The large effect of the OPL on the joint gaps might also be related to the lateral translation of the tibia as shown in Figure 9, but as it is difficult to relate the anatomical location of the OPL to its mechanical behavior during a varus or valgus movement, further research could provide more information about the role of the OPL during varus or valgus stress.

Figure 6 also shows that the change in joint gap depends on whether the reference strain in a ligament bundle was increased or decreased. Based on Figure 3, we can conclude that for a ligament to be more lax, and thus for the joint gap on the side of that ligament to be larger, the non-linear force-strain curve should be shifted to the right. This means that the slack length L_0 should be larger, which can be achieved by decreasing the reference strain, according to Equation 3. This corresponds with the results in Figure 6: decreasing the reference strain in for example the sMCL, resulted in an increased medial joint gap during a valgus laxity test (Figure 6b). Effects similar to those of the medial and lateral joint gap change as a result of changing the reference strains in medial and lateral ligaments, can be observed for the PC: changing the reference strain in the medial bundles of the PC (mPC and m_mPC)

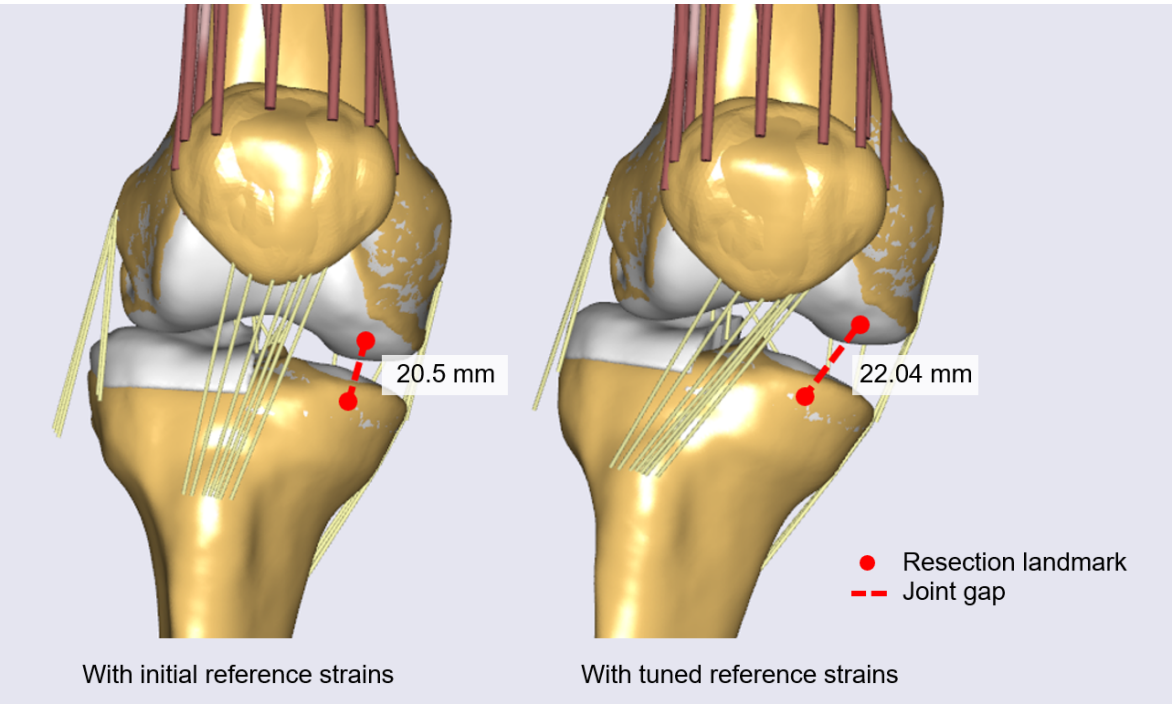

Figure 9: The medial joint gap for the modeled valgus laxity test for the initial reference strains (left) and the tuned reference strains (right).

had a larger effect on the medial joint gap during the valgus laxity test than changing the reference strain in the lateral bundles of the PC (m_lPC and lPC), as can be seen in Figure 6b. We can, however, also see that changing the reference strain in, for example, the sMCL for the valgus laxity test, had an opposite effect on the lateral joint gap as well (Figure 6a). The same applies to changes in the reference strain of lateral ligaments like the LCL and ALL, which had a small opposite effect on the medial joint gap for the varus laxity test as well (Figure 6d). These effects are likely caused by the behavior of the model: when a stress is applied, the model will look for an equilibrium, and will stop when it reaches this equilibrium. As the used MS model does not apply restrictions to certain movements so that only varus or valgus movement is allowed, it is possible that the tibia translates, for example, medially or laterally, or rotates internally or externally, after changing the reference strain of any ligament bundle. This model shifting behavior could thus cause small changes in the joint gaps where we would not necessarily expect them.

Figure 7 shows how each reference strain tuning step affected the difference between the simulated and measured joint gaps. As on both the lateral and the medial side, the measured joint gap was larger than the simulated joint gap, we can state that the joint gap itself increases when the difference between the simulated and measured joint gap decreases. The goal of the soft tissue tuning process was to reduce the difference between the simulated and measured joint gaps to reach the stopping criterion shown in Figure 2. Both Figure 7 and 8 show that the final difference between the simulated and measured joint gaps are smaller than the stopping criterion for the tuning process of 0.05 mm, as defined in Figure 2, for both the lateral and medial joint gap. While most joint gap changes during the tuning process, as described in Appendix F, were as expected, some tuning steps resulted in unexpected changes. An observation worth mentioning is that for many tuning steps, the side of the knee where ligaments were not tuned, were affected more than expected. For example, in tuning step 1, the sMCL was tuned to change the medial joint gap, but the resulting change in lateral joint gap was bigger than expected. Although the sensitivity analysis showed other results when tuning the sMCL, it is important to note that during the soft tissue tuning process, multiple ligament bundles were tuned at a time as opposed to the reference strain adaption method used during the sensitivity analysis. An explanation for this could be that when tuning one bundle of a multiple-bundle ligament, the remaining bundles of that ligament constrain gap opening, which is confirmed by the increased bundle strains of the remaining bundles as can be seen in Appendix E. Another explanation for the difference between the expected and actual change in joint gaps, is that the tuning steps were based on the same sensitivity analysis, while the sensitivity of the modeled joint gaps to changes in the reference strain might change after a tuning step.

The results of the last tuning step in Figure 7 together with the initial difference between the simulated and measured joint gaps are shown in Figure 8. From this, we can conclude that the difference between the simulated and measured joint gaps de-

creased from 1.50 mm to -0.04 mm medially, and from 1.11 mm to 0.01 mm laterally, which is an absolute decrease of 97.33% medially and 99.10% laterally. While the final simulated joint gaps are close to the intraoperatively measured joint gaps, we cannot say that the resulting movements of the model exactly match those during surgery. Figure 9 shows that beside the larger medial joint gap for the tuned situation, there was also a lateral translation and external rotation of the tibia compared to the initial situation. Comparing this to the intraoperative measurements in Figure 5, we can clearly see that the modeled tibial translation and rotation was larger than during the intraoperative laxity tests. An explanation for this is, as mentioned before, that the model does not restrict certain movements that the surgeon can, either consciously or unconsciously, reduce during the intraoperative laxity tests. Another important observation is that the strains of many ligament bundles increased for each tuning step, as shown in Appendix G. As the ligament bundle strains were initially mostly high, with some values even exceeding the yield strains, it is difficult to determine whether the resulting strain values are realistic.

4.2. Assessment of study decisions

During this study, several decisions were made, the first of which was the magnitude of the reference strain perturbations. In a previous study conducted with a similar MS model [27], the reference strain was perturbed by ± 0.06 using steps of 0.01, based on the yield strains of the ligaments. They found a maximal change in proximal-distal tibial translation of approximately -0.7 mm. As the difference between the intraoperatively measured and simulated joint gap in the present study was around two times larger, a perturbation of ± 0.1 was considered the most justified option.

The second decision was the stopping criterion. The Mako system rounds the joint gaps to zero decimals and thus a stopping criterion of 0.5 mm might have sufficed: when the gap difference goes below 0.5 mm, we cannot know whether the simulated joint gap is getting closer to or farther from the measured joint gap. Nonetheless, the choice was made to define a stopping criterion of 0.05 mm to obtain a more exact insight into the sensitivity of the model.

The third important decision was the use of joint gaps for the validation, while using the varus or valgus angle would have likely been more accurate. Intraoperatively, the surgeon uses the joint gaps during the ligament balancing phase, which is also when the measurements were done. To match this procedure, the choice was made to use the joint gaps for validating the ligament tuning process. This could affect the accuracy of the ligament tuning process, for example due to the lateral translation of the tibia observed during this study.

Lastly, the simulated joint gaps were defined as the distance between the distal resection landmark on the femur and the proximal resection landmark on the tibia, while the Mako system defines the joint gap as the distance between the femoral and tibial resection plane. It is important to note that this choice could affect the accuracy of the ligament tuning process as well.

4.3. Strengths

The main strength of this study is the comparison of the model's behavior to intraoperative measurements. In research by Tzanetis et al. [12] [23], the lack of model validation using experimental measurements was a considerable limitation. Evaluating the ability of the model to replicate intraoperatively measured knee laxities could contribute to further enhancing the model to eventually implement a real-time model in the RA-TKA workflow. Besides, the measurement protocol and database resulting from this study and the used research methods form a foundation for possible additional soft tissue tuning and thus further validation of the model.

4.4. Limitations and further research

The present study has some limitations. First, the present study attempts to optimize an underdetermined system. Therefore, there are multiple possible solutions. Second, only one research subject was included, and only the pre-implant situation for 0° flexion was used for the sensitivity analysis and soft-tissue tuning. While the intraoperative laxity measurements were done for four subjects, one subject was included to evaluate the ability of the model to replicate intraoperatively measured laxity values. For increased personalization of the resulting tuned model, the methods described for this study should be repeated for 90° flexion and for the post-implant situation, for which the implant should be added to the model according to the final implant positioning. Third, the force applied to the knee during the intraoperative varus and valgus laxity tests is unknown: the surgeon applied a force until he felt, in his opinion, enough resistance. [11] As the simulated joint gaps and thus also the soft-tissue tuning process depend greatly on the applied force, as shown in Appendix A, measuring the intraoperatively applied force, for example with a force-measuring spacer as proposed by Wang et al. [37], may be of added value for possible future comparable measurements. Besides, both the intraoperative force application and the soft tissue balancing process are operator dependent, which may affect the measurement values. Fourth, the model has no restrictions to certain movements, leading to model shifting characterized by increased translation and external or internal rotation of the tibia. Therefore, the simulated laxity values might be less accurate. Intraoperatively, the surgeon can (un)consciously stabilize the knee to prevent these kinds of movements. Looking into ways to add such movement restrictions to the model may

be of added value. Fifth, we cannot neglect that many ligament bundle strain values in the model were large and sometimes exceeded their yield strains [23], especially for the dMCL, pPCL and the medial bundles of the PC for the valgus tests, and for the ACL and ALL for the varus tests, as can be seen in Appendix E and G. This makes it difficult to determine whether the joint gap and strain values resulting from the nine tuning steps are realistic. In order to evaluate the accuracy of the resulting joint gaps and ligament strains, assessing the behaviour of the modeled ligaments could be of added value. Sixth, the sensitivity analysis was only done once before the soft-tissue tuning process and the reference strain of each ligament bundle was perturbed separately. This may have caused a difference between the expected and actual joint gap change for each tuning step. A more precise method would be to conduct a sensitivity analsyis after each tuning step and base the next tuning step on the resulting sensitivities of the previous step. Furthermore, the tuning process was done manually. While the final simulated joint gaps are close to the intraoperatively measured values, there are possibly many combinations of reference strains that would result in similar joint gap values. The optimal combination of reference strains could be found by doing a proper optimization process. Finally, the used MS model has its own limitations, for example the fact that it does not include the menisci, and it does not simulate the behaviour of the articular cartilage of the knee, which could have lead to a less stable knee joint and increased ligament strains. [23]

5. Conclusion

In summary, the soft tissue in this particular CT-based personalized MS model could be tuned to the extent that the differences between the simulated and intraoperatively measured joint gaps are -0.04 (0.18%) medially and 0.01 (0.04%) laterally. This was achieved by performing intraoperative varus and valgus laxity measurements, conducting a sensitivity analysis of the personalized MS model by perturbing the reference strains of the individual ligament bundles, and performing a manual soft-tissue tuning process where ligaments reference strains were tuned step-by-step. An automated optimization process may contribute to a more optimal combination of reference strains to achieve similar results. The ability to reduce the difference between the measured and simulated joint gaps in this study suggests that the model could be usable for pre-planning of TKA procedures in the future, although multiple aspects still need to be adjusted or added to the model, and a more extensive validation of the model against intraoperative is needed. Although we were able to minimize the difference between the measured and simulated joint gaps, the main conclusion thus remains that further work is required to eventually implement the model clinically.

References

[1] F. Mancino, G. Cacciola, M. A. Malahias, R. De Filippis, D. De Marco, V. Di Matteo, A. Gu, P. K. Sculco, G. Maccauro, and I. De Martino, "What are the benefits of robotic-assisted total knee arthroplasty over conventional manual total knee arthroplasty? A systematic review of comparative studies," *Orthopedic Reviews*, vol. 12, pp. 15–22, jun 2020.

[2] J. Mitchell, J. Wang, B. Bukowski, J. Greiner, B. Wolford, M. Oyer, and R. L. Illgen, "Relative Clinical Outcomes Comparing Manual and Robotic-Assisted Total Knee Arthroplasty at Minimum 1-Year Follow-up," *HSS Journal*, vol. 17, pp. 267–273, oct 2021.

[3] J. Zhang, ·. Wofhatwa, S. Ndou, N. Ng, P. Gaston, P. M. Simpson, G. J. Macpherson, J. T. Patton, and N. D. Clement, "Robotic-arm assisted total knee arthroplasty is associated with improved accuracy and patient reported outcomes: a systematic review and meta-analysis Minimal clinical important difference," *Knee Surgery, Sports Traumatology, Arthroscopy*, vol. 30, pp. 2677–2695, 2022.

[4] E. L. Hampp, M. Chughtai, L. Y. Scholl, N. Sodhi, M. Bhowmik-Stoker, D. J. Jacofsky, and M. A. Mont, "Robotic-Arm Assisted Total Knee Arthroplasty Demonstrated Greater Accuracy and Precision to Plan Compared with Manual Techniques," *Journal of Knee Surgery*, vol. 32, pp. 239–250, 2019.

[5] N. Agarwal, K. To, M. BChir Dip Clin Ed, S. McDonnell, F. Tra, W. Khan, and D. Clin Ed, "Systematic Review and Meta-Analysis Clinical and Radiological Outcomes in Robotic-Assisted Total Knee Arthroplasty: A Systematic Review and Meta-Analysis," *Journal of Arthroplasty*, 2020.

[6] C. Batailler, A. Fernandez, J. Swan, ·. E. Servien, ·. Fares, S. Haddad, F. Catani, S. Lustig, E. Servien, and F. S. Haddad, "MAKO CT-based robotic arm-assisted system is a reliable procedure for total knee arthroplasty: a systematic review," *Knee Surgery, Sports Traumatology, Arthroscopy*, vol. 29, pp. 3585–3598, 2021.

[7] S. A. Ofa, B. J. Ross, T. R. Flick, A. H. Patel, and W. F. Sherman, "Robotic Total Knee Arthroplasty vs Conventional Total Knee Arthroplasty: A Nationwide Database Study," *Arthroplasty Today*, 2020.

[8] Stryker, "MAKO TKA Surgical Guide."

[9] A. Ensini, F. Zambianchi, A. Illuminati, and F. Catani, "Isolated patellofemoral (PFJ) and biunicompartmental (BIUKA) makoplasty," in *Robotic surgery for total hip and knee replacement*, ch. 5.2, 2019.

[10] J. Bellemans, W. Colyn, H. Vandenneucker, and J. Victor, "The Chitranjan Ranawat Award Is Neu-

tral Mechanical Alignment Normal for All Patients? The Concept of Constitutional Varus," *Clinical Orthopaedics and Related Research*.

[11] F. Zambianchi, G. Bazzan, A. Marcovigi, M. Pavesi, A. Illuminati, A. Ensini, and F. Catani, "Joint line is restored in robotic-arm-assisted total knee arthroplasty performed with a tibia-based functional alignment," *Archives of Orthopaedic and Trauma Surgery*, vol. 141, pp. 2175–2184, dec 2021.

[12] P. Tzanetis, R. Fluit, K. de Souza, S. Robertson, B. Koopman, and N. Verdonschot, "Pre-Planning the Surgical Target for Optimal Implant Positioning in Robotic-Assisted Total Knee Arthroplasty," *Bioengineering 2023, Vol. 10, Page 543*, vol. 10, p. 543, apr 2023.

[13] H. D. Rajgor, A. Mayne, C. Munasinghe, J. Pagkalos, Y. Agrawal, E. T. Davis, and A. D. Sharma, "Mako versus ROSA: comparing surgical accuracy in robotic total knee arthroplasty," *Journal of Robotic Surgery*, vol. 18, pp. 1–5, dec 2024.

[14] J. D. Sires, J. D. Craik, and C. J. Wilson, "Accuracy of Bone Resection in MAKO Total Knee Robotic-Assisted Surgery," *Journal of Knee Surgery*, vol. 34, pp. 745–748, jun 2021.

[15] L. Bartsoen, M. G. Faes, R. Wirix-Speetjens, D. Moens, I. Jonkers, and J. V. Sloten, "Probabilistic planning for ligament-balanced TKA-Identification of critical ligament properties," *Frontiers in bioengineering and biotechnology*, vol. 10, nov 2022.

[16] M. A. Marra, V. Vanheule, R. Fluit, B. H. Koopman, J. Rasmussen, N. Verdonschot, and M. S. Andersen, "A subject-specific musculoskeletal modeling framework to predict in vivo mechanics of total knee arthroplasty," *Journal of biomechanical engineering*, vol. 137, feb 2015.

[17] M. Kebbach, M. Darowski, S. Krueger, C. Schilling, T. M. Grupp, R. Bader, and A. Geier, "materials Musculoskeletal Multibody Simulation Analysis on the Impact of Patellar Component Design and Positioning on Joint Dynamics after Unconstrained Total Knee Arthroplasty," *Materials*.

[18] Q. Zhang, N. C. Adam, S. H. Hosseini Nasab, W. R. Taylor, and C. R. Smith, "Techniques for In Vivo Measurement of Ligament and Tendon Strain: A Review," *Annals of Biomedical Engineering*, vol. 49, pp. 7–28, jan 2021.

[19] H. Naghibi, V. Mazzoli, K. Gijsbertse, G. Hannink, A. Sprengers, D. Janssen, T. Van den Boogaard, and N. Verdonschot, "A noninvasive MRI based approach to estimate the mechanical properties of human knee ligaments," *Journal of the Mechanical Behavior of Biomedical Materials*, vol. 93, pp. 43–51, may 2019.

[20] W. T. Wilson, A. H. Deakin, A. P. Payne, F. Picard, and S. C. Wearing, "Comparative analysis of the structural properties of the collateral ligaments of the human knee," *Journal of Orthopaedic and Sports Physical Therapy*, vol. 42, pp. 345–351, apr 2012.

[21] J. R. Robinson, A. M. Bull, and A. A. Amis, "Structural properties of the medial collateral ligament complex of the human knee," *Journal of Biomechanics*, vol. 38, pp. 1067–1074, may 2005.

[22] J. A. Ewing, M. K. Kaufman, E. E. Hutter, J. F. Granger, M. D. Beal, S. J. Piazza, and R. A. Siston, "Estimating patient-specific soft-tissue properties in a TKA knee," *Journal of Orthopaedic Research*, vol. 34, pp. 435–443, mar 2016.

[23] P. Tzanetis, K. de Souza, S. Robertson, R. Fluit, B. Koopman, and N. Verdonschot, "Numerical study of osteophyte effects on pre-operative knee functionality in patients undergoing total knee arthroplasty," 2022.

[24] Stryker, "MAKO TKA Application User Guide."

[25] L. Blankevoort, J. H. Kuiper, R. Huiskes, and H. J. Grootenboer, "Articular contact in a three-dimensional model of the knee," *Journal of biomechanics*, vol. 24, no. 11, pp. 1019–1031, 1991.

[26] J. Wismans, F. Veldpaus, J. Janssen, A. Huson, and P. Struben, "A THREE-DIMENSIONAL MATHEMATICAL MODEL OF THE KNEE-JOINT*," *Journal of Biomechanics*, vol. 13, pp. 677–685.

[27] F. Kerkhof, *Sensitivity of passive knee extension secondary tibiofemoral kinematics to ligament stiffness and reference strain.* PhD thesis, University of Twente, 2021.

[28] D. L. Butler, K. D. Maithew, and D. C. Stouffer, "COMPARISON OF MATERIAL PROPERTIES IN FASCICLE-BONE UNITS FROM HUMAN PATELLAR TENDON AND KNEE LIGAMENTS," *Journal of Biomechanics*.

[29] J. R. Robinson, A. M. Bull, R. R. W. Thomas, and A. A. Amis, "The role of the medial collateral ligament and posteromedial capsule in controlling knee laxity," *American Journal of Sports Medicine*, vol. 34, pp. 1815–1823, nov 2006.

[30] W. P. Seering, R. L. Piziali, D. A. Nagel, and D. J. Schurman, "The function of the primary ligaments of the knee in varus-valgus and axial rotation," *Journal of Biomechanics*, vol. 13, pp. 785–794, jan 1980.

[31] S. T. Swinford, R. Laprade, L. Engebretsen, M. Cohen, and M. Safran, "Biomechanics and physical examination of the posteromedial and posterolateral knee: state of the art," *Journal of ISAKOS*, vol. 5, pp. 378–388, nov 2020.

[32] T. Miyasaka, H. Matsumoto, Y. Suda, T. Otani, and Y. Toyama, "Coordination of the anterior and posterior cruciate ligaments in constraining the

varus–valgus and internal–external rotatory instability of the knee," *Journal of Orthopaedic Science*, vol. 7, pp. 348–353, may 2002.

[33] S. Ball, J. M. Stephen, H. El-Daou, A. Williams, and A. A. Amis, "The medial ligaments and the ACL restrain anteromedial laxity of the knee," *Knee Surgery, Sports Traumatology, Arthroscopy*, vol. 28, pp. 3700–3708, dec 2020.

[34] M. Inoue, E. Mcgurk-Burleson, J. M. Hollis, and S. L. Woo, "Treatment of the medial collateral ligament injury," *The American Journal of Sports Medicine*, vol. 15, pp. 15–21, jan 1987.

[35] V. MEHTA, P. DAWANI, and P. GOEL, "Morphologic and Morphometric Evaluation of Oblique Popliteal Ligament - A Clinico-Anatomical Study," *Mædica*, vol. 17, p. 641, sep 2022.

[36] P. M. Morgan, R. F. Laprade, F. A. Wentorf, J. W. Cook, and A. Bianco, "The Role of the Oblique Popliteal Ligament and Other Structures in Preventing Knee Hyperextension," *American Journal of Sports Medicine*, vol. 38, pp. 550–557, mar 2010.

[37] F.-X. Wang, Z.-Y. Wu, Q.-H. Lin, T. Chen, S.-L. Kuang, M.-F. Gan, L.-X. Huang, and L.-N. Sun, "Novel Force Measurement System for Soft Tissue Balance in Total Knee Arthroplasty Based on Flexible Pressure Sensor Arrays," *Advanced Intelligent Systems*, vol. 4, p. 2100156, apr 2022.

A. Force magnitude

As the intraoperatively applied varus and valgus force is unknown, the force magnitude in the MS model was determined by conducting a small sensitivity analysis. The force magnitude was perturbed from 10 N to 100 N, obtaining the lateral and medial joint gaps, as well as the strains of the bundles of the dMCL, when applying a valgus stress. This way, the effect of changing the force magnitude on the joint gaps and the dMCL strain could be observed. The dMCL was selected for this analysis, because this ligament showed the highest strains when running the model with its initial force settings for a neutral laxity test with no varus or valgus stress, but with the tibial offset simulating the surgical spoon. Figure A.1 shows the resulting force-laxity curves, and Figure A.2 shows the resulting force-strain curves.

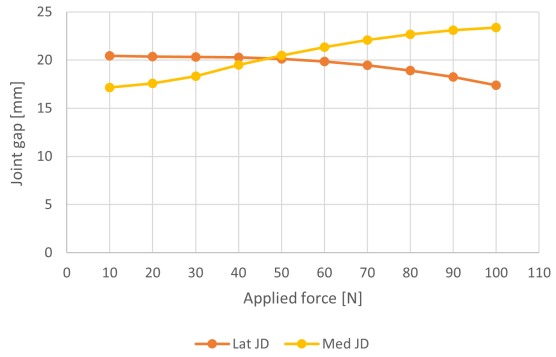

Figure A.1: The medial and lateral joint gaps for different applied valgus forces

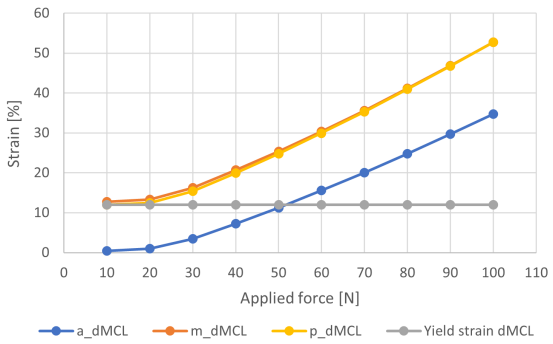

Figure A.2: The strains in the three dMCL bundles for different applied valgus forces

Figure A.1 shows that the force magnitude has a small effect on the joint gaps. Figure A.2 shows that for higher forces, the strain of the dMCL is higher, and the strain is more sensitive to changes in the force. For lower forces, the strain of the dMCL decreased for all bundles, with a near constant strain for forces close to 10 N. The curve also shows that the medial and posterior bundles of the dMCL had a prestrain of approximately 12%, which is also the yield strain of the dMCL. The strain of the anterior dMCL bundle was lower than the yield strain for forces equal to and lower than approximately 50 N. These findings, together with the fact that for forces lower than 50 N the joint gaps opened up minimally during a simulated valgus or varus laxity test, were reason to select an applied force of 50 N.

B. Joint gap redefinition

In the original MS model, the joint gap was defined as the distance between the anatomical frames of the femur and the tibia. As the measurements were done for the medial and lateral joint gap seperately, the joint gap definition of the model was adapted. Instead of one joint gap, two separate joint gaps were defind to simulate the medial and lateral joint gaps. For this, the femoral and tibial resection landmarks were used. These landmarks originally are located on the contact surfaces of the femur and tibia. However, the Mako ® system defins the medial and lateral joint gaps as the distance between the resected bones of the medial femoral epicondyle and medial tibial condyle, and between the resected bones of the lateral femoral epicondyle and lateral tibial condyle, respectively. Therefore, the planned resection depths were subtracted from the femoral and tibial resection landmarks. To clarify this concept, Figure B.1 schematically shows the joint gap definition.

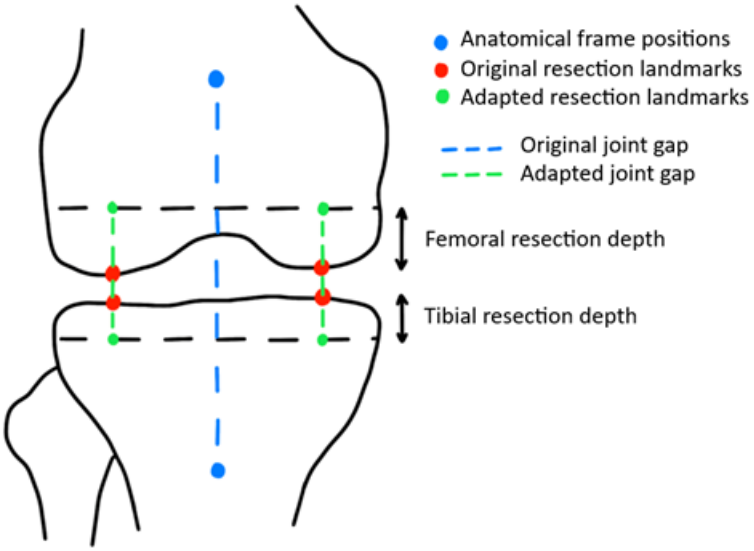

Figure B.1: Schematic visualization of redefining the joint gap in the MS model

The adapted resection landmarks were converted to moving frames, so their coordinates change as the model moves. As the joint gaps are used as an implication whether the implant will eventually fit between the osteotomies during surgery, according to its thickness, it was assumed that subtracting the resection depth from only the y-coordinates of the resection landmarks, as opposed to using the Euclidian distance, was accuracte enough to simulate the intraoperative joint gaps.

C. Python script

The Python script used for the sensitivity analysis can be found below. The original code is longer as it includes both the varus and valgus laxity tests, and all ligaments. The code below was adapted to serve as an example for the valgus laxity test for the ACL.

```
# -*- coding: utf-8 -*-
"""
Created on Wed Apr  3 17:25:32 2024

@author: irism
"""

# Import packages:
import numpy as np
from anypytools import AnyMacro
from anypytools import AnyPyProcess
from anypytools.macro_commands import (Load, SetValue, Dump, OperationRun, SaveData)
from scipy.io import savemat

# Important: in AnyBody manually:
# 1) uncomment only the laxity test you want to run & save file (LaxityStudiesClass.any)
# 2) change knee angle to 90 for flexion tests & save file (LaxityStudyClass.any)

# Important: manually copy the resulting .mat output files to MATLAB folder to be able to load them
 ↪  in MATLAB

# Define paths for exporting joint distractions
LateralJointDistraction = 'Main.KneeFDKModel.Right.SelectedOutput.JointKinematics.TibiaFemurKinemat
 ↪  ics.LateralJointDistraction';
MedialJointDistraction = 'Main.KneeFDKModel.Right.SelectedOutput.JointKinematics.TibiaFemurKinemati
 ↪  cs.MedialJointDistraction';

# Define paths for exporting strains
strain_ACL = 'Main.KneeFDKModel.Right.Ligaments.ACL.eps'
strain_PCL = 'Main.KneeFDKModel.Right.Ligaments.PCL.eps'
strain_OPL = 'Main.KneeFDKModel.Right.Ligaments.OPL.eps'
strain_PC = 'Main.KneeFDKModel.Right.Ligaments.PC.eps'
strain_sMCL = 'Main.KneeFDKModel.Right.Ligaments.sMCL.eps'
strain_dMCL = 'Main.KneeFDKModel.Right.Ligaments.dMCL.eps'
strain_LCL = 'Main.KneeFDKModel.Right.Ligaments.LCL.eps'
strain_ALL = 'Main.KneeFDKModel.Right.Ligaments.ALL.eps'

# After this point: run each collapsible section entirely to avoid confusion due to overwriting of
 ↪  outcome variables!!!

#%% Define some sets of initial conditions for the joint position the model can try:
init_cond_1 = np.array([0,0,0,0,0]);
init_cond_2 = np.array([1.685639254544086e-03, 1.451904535198226e-03, 8.766829572166876e-04,
 ↪  1.454370826916984e-02, -1.088302717758660e-02]);
init_cond_3 = np.array([1.874397919427273e-03, 1.428633985080691e-03, 8.910117475130711e-04,
 ↪  7.181274922905767e-03, -1.657736634858453e-02]);
init_cond_4 = np.array([2.030606020000246e-03, 1.394672496094991e-03, 9.004258140939661e-04,
 ↪  3.361432623698202e-03, -1.969556080479057e-02]);
init_cond_5 = np.array([2.357065457329972e-03, 1.313576260723251e-03, 9.332075653755363e-04,
 ↪  -2.092708892603989e-03, -2.484658838280790e-02]);
init_cond_6 = np.array([2.552524624370683e-03, 1.272658825690366e-03, 1.162066871069336e-03,
 ↪  -3.583614663465045e-03, -2.897248210641742e-02]);
init_cond_7 = np.array([2.923019368322211e-03, 1.249416063747946e-03, 1.115267230192608e-03,
 ↪  -4.973634021858103e-03, -3.282675117852801e-02]);
init_cond_8 = np.array([3.044487901122683e-03, 1.249425065758107e-03, 1.090980955552216e-03,
 ↪  -5.098237391833653e-03, -3.373530012180311e-02]);
init_cond_9 = np.array([3.244441352431979e-03, 1.257480685110909e-03, 1.058920453485084e-03,
 ↪  -4.757507907546338e-03, -3.503698430664487e-02]);
init_cond_10 = np.array([3.573153608002259e-03, 1.272455924266880e-03, 9.571965461172584e-04,
 ↪  -3.822974944428625e-03, -3.629774969509919e-02]);
init_cond_11 = np.array([3.916866261717079e-03, 1.277949088317963e-03, 8.159968225500804e-04,
 ↪  -2.748766597406749e-03, -3.758362397320755e-02]);
init_cond_12 = np.array([4.143369376065686e-03, 1.275084306780898e-03, 7.039439681650378e-04,
 ↪  -1.915136077341894e-03, -3.844557865270980e-02]);
init_cond_13 = np.array([4.343142593747217e-03, 1.263972657921316e-03, 5.855728406281937e-04,
 ↪  -1.040628510957098e-03, -3.924603727297538e-02]);
init_cond_14 = np.array([4.436258611111818e-03, 1.255529335333483e-03, 5.143312187426087e-04,
 ↪  -5.695593691257271e-04, -3.955939079687538e-02]);
```

```
init_cond_15 = np.array([4.673259681897372e-03, 1.219869827208304e-03, 3.185775260632130e-04,
↪  9.617104808307686e-04, -4.050043813077352e-02]);
init_cond_16 = np.array([4.918024849951104e-03, 1.162110269866465e-03, 1.196041420538439e-05,
↪  3.479828082556257e-03, -4.100828428564487e-02]);
init_cond_17 = np.array([5.114132375042825e-03, 8.941270449661174e-04, -9.559768514052513e-04,
↪  8.757916929859997e-03, -3.040733339693739e-02]);
init_cond_18 = np.array([5.084291618535695e-03, 8.617939402422400e-04, -1.067120375083010e-03,
↪  9.216708407448149e-03, -2.886206703669718e-02]);
init_cond_19 = np.array([5.013061510484013e-03, 7.936994497288645e-04, -1.393297138639097e-03,
↪  1.036998327834279e-02, -2.847153102535019e-02]);
init_cond_20 = np.array([4.999253454945594e-03, 7.794657589376671e-04, -1.618487363399494e-03,
↪  1.092507735710660e-02, -2.847983579952149e-02]);

# Create matrix of intial conditions sets for looping:
init_cond = [init_cond_1, init_cond_2, init_cond_3, init_cond_4, init_cond_5,
             init_cond_6, init_cond_7, init_cond_8, init_cond_9, init_cond_10,
             init_cond_11, init_cond_12, init_cond_13, init_cond_14, init_cond_15,
             init_cond_16, init_cond_17, init_cond_18, init_cond_19, init_cond_20]

# Define first initial conditions index:
start = 0

#%% Example sensitivity analysis for 'extension valgus' for 'ACL'

# Important: For other ligaments, replace 'ACL' in the variation arrays and matrices with the
↪  correct ligament and change the array and matrix sizes if needed

# Important: For varus, replace 'valgus' with 'varus'

# Initialize output arrays for joint distraction:
lat_joint_dist = np.zeros(4); med_joint_dist = np.zeros(4)

# Initialize output matrices for individual ligament bundle strains (rows = perturbations, columns
↪  = ligament bundles):
eps_ACL = np.zeros((4,2)); eps_PCL = np.zeros((4,2)); eps_OPL = np.zeros((4,1)); eps_PC =
↪  np.zeros((4,4));
eps_sMCL = np.zeros((4,3)); eps_dMCL = np.zeros((4,3)); eps_LCL = np.zeros((4,3)); eps_ALL =
↪  np.zeros((4,2))

# Initial reference strain values for ligament bundles:
epsr_ACL_1 = 0.35;    epsr_ACL_2 = 0.35

# Create arrays of the variations of the reference strains (initial +/- 0.1):
steps_ACL_1 = [epsr_ACL_1 - 0.1 , epsr_ACL_1 , epsr_ACL_1 + 0.1]
steps_ACL_2 = [epsr_ACL_2 - 0.1 , epsr_ACL_2 , epsr_ACL_2 + 0.1]

# Create matrices of the variations of the reference strains:
epsr_ACL = [np.array([steps_ACL_1[0], steps_ACL_2[1]]), # bundle 1 -0.1
           np.array([steps_ACL_1[2], steps_ACL_2[1]]), # bundle 1 +0.1
           np.array([steps_ACL_1[1], steps_ACL_2[0]]), # bundle 2 -0.1
           np.array([steps_ACL_1[1], steps_ACL_2[2]])] # bundle 2 +0.1

# Run simulation:
for i in range(len(epsr_ACL)):
    epsr_ACL_i = epsr_ACL[i] # define epsr variation

    macrolist_ACL = [
    [Load('takom_pers_exp_version_ext\Application\Model\S04\Osteophytes-free\Main.any'),

    # SetValue to try initial conditions:
    SetValue('Main.KneeFDKModel.Right.JntFDK.TibiaFemurJointFDK.DriverPos0', init_cond[start]),
    # SetValue espr (reference strain) for ligaments bundles:
    SetValue('Main.KneeFDKModel.Right.ModelParameters.Ligaments.ACL.epsr', epsr_ACL_i),
    OperationRun('Main.RunAndSaveLigamentCalibration'),
    OperationRun('Main.RunLaxityStudies'),
    Dump(LateralJointDistraction),
    Dump(MedialJointDistraction),
    Dump(strain_ACL),
    Dump(strain_PCL),
    Dump(strain_OPL),
    Dump(strain_PC),
    Dump(strain_sMCL),
    Dump(strain_dMCL),
    Dump(strain_LCL),
    Dump(strain_ALL),
```

```
    ]]

    app = AnyPyProcess()

    try: results_ACL = app.start_macro(macrolist_ACL) # try to run macro with first set of initial
     ↪  conditions
    except: start += 1 # use next set of initial conditions and try again

    lat_joint_dist[i] = results_ACL[0][LateralJointDistraction]
    med_joint_dist[i] = results_ACL[0][MedialJointDistraction]

    eps_ACL[i] = results_ACL[0][strain_ACL]
    eps_PCL[i] = results_ACL[0][strain_PCL]
    eps_OPL[i] = results_ACL[0][strain_OPL]
    eps_PC[i] = results_ACL[0][strain_PC]
    eps_sMCL[i] = results_ACL[0][strain_sMCL]
    eps_dMCL[i] = results_ACL[0][strain_dMCL]
    eps_LCL[i] = results_ACL[0][strain_LCL]
    eps_ALL[i] = results_ACL[0][strain_ALL]

# Create list of output variables:
output_ACL_ext_valgus = [lat_joint_dist, med_joint_dist, eps_ACL, eps_PCL, eps_OPL, eps_PC,
                         eps_sMCL, eps_dMCL, eps_LCL, eps_ALL]

# Save output variables as .mat file:
FrameStack_ACL_ext_valgus = np.empty((len(output_ACL_ext_valgus),), dtype=np.object)
for i in range(len(output_ACL_ext_valgus)):
    FrameStack_ACL_ext_valgus[i] = output_ACL_ext_valgus[i]
savemat("output_ACL_ext_valgus.mat", {"FrameStack":FrameStack_ACL_ext_valgus})
```

D. Measurement data

The measurement data was collected by taking videos of the Mako screen, which were later processed into an Excel sheet, as shown below. The data of TKA subject 3 was used for this study.

TKA subject 1:

Pre-implant				
No stress	Actual angle (deg)	Varus (deg)	Joint gap lat. (mm)	Joint gap med. (mm)
0 deg	6	10	17	11
90 deg	90	4	17	13
Varus stress	Actual angle (deg)	Varus (deg)	Joint gap lat. (mm)	Joint gap med. (mm)
0 deg	7	14	18	8
90 deg	91	6	18	x*
Valgus stress	Actual angle (deg)	Varus (deg)	Joint gap lat. (mm)	Joint gap med. (mm)
0 deg	9	3	17	16
90 deg	91	6	x*	14

*These cannot be measured, as for 90 degrees knee flexion, we cannot do valgus stress and varus stress seperately: the surgeon places a spoon below the femur on both the lateral and medial side and then applies stress, so the gap opens up simultaneously medial and lateral. In this case, the laxity is |17-18| = 1 mm laterally and |13-14| = 1 mm

Post-implant				
No stress	Actual angle (deg)	Varus (deg)	Joint gap lat. (mm)	Joint gap med. (mm)
0 deg	0	7	20	18
90 deg	89	6	20	19
No stress	Actual angle (deg)	Varus (deg)	Joint gap lat. (mm)	Joint gap med. (mm)
0 deg	1	8	21	18
90 deg	92	7	22	19
No stress	Actual angle (deg)	Varus (deg)	Joint gap lat. (mm)	Joint gap med. (mm)
0 deg	0	5	19	19
90 deg	88	5	20	20

TKA subject 2:

Pre-implant				
No stress	Actual angle (deg)	Varus (deg)	Joint gap lat. (mm)	Joint gap med. (mm)
0 deg	10	6	19	12
90 deg	93	1	17	13
Varus stress	Actual angle (deg)	Varus (deg)	Joint gap lat. (mm)	Joint gap med. (mm)
0 deg	10	7	19	11
90 deg	92	5	19	x*
Valgus stress	Actual angle (deg)	Varus (deg)	Joint gap lat. (mm)	Joint gap med. (mm)
0 deg	10	3	19	14
90 deg	92	1	x*	14

*These cannot be measured, as for 90 degrees knee flexion, we cannot do valgus stress and varus stress seperately: the surgeon places a spoon below the femur on both the lateral and medial side and then applies stress, so the gap opens up simultaneously medial and lateral. In this case, the laxity is |18-19| = 1 mm laterally and |13-14| = 1 mm

Post-implant				
No stress	Actual angle (deg)	Varus (deg)	Joint gap lat. (mm)	Joint gap med. (mm)
0 deg	3	1	17	18
90 deg	90	2	18	18
No stress	Actual angle (deg)	Varus (deg)	Joint gap lat. (mm)	Joint gap med. (mm)
0 deg	5	3	20	18
90 deg	91	5	21	18
No stress	Actual angle (deg)	Varus (deg)	Joint gap lat. (mm)	Joint gap med. (mm)
0 deg	4	0	17	18
90 deg	91	2	18	18

TKA subject 3:

Pre-implant				
No stress	Actual angle (deg)	Varus (deg)	Joint gap lat. (mm)	Joint gap med. (mm)
0 deg	3	3	22	20
90 deg	90	1	18	18
Varus stress	Actual angle (deg)	Varus (deg)	Joint gap lat. (mm)	Joint gap med. (mm)
0 deg	4	9	23	17
90 deg	89	3	20	x*
Valgus stress	Actual angle (deg)	Varus (deg)	Joint gap lat. (mm)	Joint gap med. (mm)
0 deg	2	2	21	22
90 deg	89	3	x*	19

*These cannot be measured, as for 90 degrees knee flexion, we cannot do valgus stress and varus stress seperately: the surgeon places a spoon below the femur on both the lateral and medial side and then applies stress, so the gap opens up simultaneously medial and lateral. In this case, the laxity is |18-20| = 2 mm laterally and |18-19| = 1 mm

Post-implant				
No stress	Actual angle (deg)	Varus (deg)	Joint gap lat. (mm)	Joint gap med. (mm)
0 deg	0	1	19	18
90 deg	92	3	20	20
Varus stress	Actual angle (deg)	Varus (deg)	Joint gap lat. (mm)	Joint gap med. (mm)
0 deg	0	4	20	18
90 deg	92	2	20	20
Valgus stress	Actual angle (deg)	Varus (deg)	Joint gap lat. (mm)	Joint gap med. (mm)
0 deg	1	0	18	19
90 deg	93	2	20	20

TKA subject 4:

Pre-implant				
No stress	Actual angle (deg)	Varus (deg)	Joint gap lat. (mm)	Joint gap med. (mm)
0 deg	10	13	20	13
90 deg	92	8	17	13
Varus stress	Actual angle (deg)	Varus (deg)	Joint gap lat. (mm)	Joint gap med. (mm)
0 deg	13	16	22	11
90 deg	91	10	19	x*
Valgus stress	Actual angle (deg)	Varus (deg)	Joint gap lat. (mm)	Joint gap med. (mm)
0 deg	12	7	19	15
90 deg	92	6	x*	15

*These cannot be measured, as for 90 degrees knee flexion, we cannot do valgus stress and varus stress seperately: the surgeon places a spoon below the femur on both the lateral and medial side and then applies stress, so the gap opens up simultaneously medial and lateral. In this case, the laxity is |17-19| = 2 mm laterally and |13-15| = 2 mm

Post-implant				
No stress	Actual angle (deg)	Varus (deg)	Joint gap lat. (mm)	Joint gap med. (mm)
0 deg	1	5	16	17
90 deg	91	6	17	17
No stress	Actual angle (deg)	Varus (deg)	Joint gap lat. (mm)	Joint gap med. (mm)
0 deg	5	8	18	16
90 deg	91	4	17	18
No stress	Actual angle (deg)	Varus (deg)	Joint gap lat. (mm)	Joint gap med. (mm)
0 deg	4	3	16	18
90 deg	89	10	21	17

E. Sensitivity analysis results

Valgus stress:

Varus stress:

Green = decrease | Red = increase | 0-25% | 26-50% | 51-75% | 76-100% | Failed | Failed but values seem OK

Ligament	Bundle	Reference strains*																						
		epsr	Joint gaps [mm] (+/- difference from initial value)		Strain [%] (+/- difference from initial strain)																			
		-0.1	Lat	Med	aACL	pACL	aPCL	pPCL	OPL	mPC	m_mPC	l_mPC	IPC	a_dMCL	m_dMCL	p_dMCL	a_sMCL	m_sMCL	p_sMCL	aLCL	mLCL	pLCL	aALL	pALL
ACL	a	0.25	0.03	-0.02	-6.41	1.76	0	-0.71	0	-0.3	-0.41	-0.21	0.12	0	-1.53	-1.6	-0.16	-0.17	-0.17	-0.13	-0.14	-0.15	0.53	0.57
	p	0.25	0.03	0	1.95	-7.43	0	-0.63	0.07	-0.24	-0.34	-0.17	0.12	0	-1.36	-0.43	-0.11	-0.12	-0.12	-0.08	-0.09	-0.11	0.42	0.45
PCL	a	-0.56	0	0	0	0	0	0	0	0	0	0	0	0	0	0	0	0	0	0	0	0	0	0
	p	-0.13	0.17	0.06	-0.58	-0.46	0	-10.32	-0.38	0.49	0.5	0.46	0.2	0	1.72	1.86	0.21	0.22	0.25	0.28	0.29	0.31	0.34	0.34
OPL		0	-0.73	-0.12	1.77	1.83	0	-5.63	-7.11	-1.95	-1.52	-1.29	-0.27	0	-5.99	-5.67	-0.53	-0.64	-0.75	0.05	0.03	-0.05	-1.92	-1.99
PC**	m	-0.03	0.03	0.1	-0.39	-0.29	0	0.8	-0.13	-10.2	0.57	0.12	-0.07	0	1.96	2.02	0.32	0.33	0.34	-0.19	-0.2	-0.2	0.01	0.01
	m_m	-0.03	0.03	0.06	-0.37	-0.28	0	0.54	-0.06	0.38	-9.41	0.1	-0.03	0	1.33	1.36	0.19	0.2	0.21	-0.08	-0.09	-0.08	0.02	0.01
	l_m	-0.03	0.16	0.02	-0.23	-0.16	0	0.68	-0.15	0.1	0.14	-10.75	0.31	0	0.34	0.41	0.01	0.01	0.02	0.47	0.48	0.5	0.36	0.36
	l	-0.03	0.14	-0.01	0.21	0.18	0	0.28	-0.06	-1.09	-0.05	0.29	-10.46	0	-0.33	-0.3	-0.09	-0.09	-0.08	0.44	0.45	0.46	0.39	0.4
dMCL	a	-0.27	0	0	0	0	0	0	0	0	0	0	0	0	0	0	0	0	0	0	0	0	0	0
	m	-0.16	0.02	0.04	-0.36	-0.29	0	0.49	-0.09	0.34	0.35	0.07	-0.05	0	-5.99	1.32	0.16	0.17	0.18	-0.12	-0.13	-0.12	0.02	0.02
	p	-0.16	0.02	0.04	-0.34	-0.27	0	0.48	-0.1	0.32	0.33	0.07	-0.04	0	1.19	-5.67	0.15	0.16	0.17	-0.1	-0.1	-0.1	0.03	0.03
sMCL	a	-0.09	0	0.01	-0.04	-0.02	0	0.07	0	0.06	0.06	0	-0.01	0	0.17	0.18	-3.96	0.03	0.04	-0.02	-0.03	-0.03	-0.02	-0.02
	m	-0.09	0	0.01	-0.03	-0.02	0	0.07	0	0.06	0.05	0	-0.01	0	0.17	0.17	0.03	-3.75	0.04	-0.02	-0.03	-0.03	-0.01	-0.01
	p	-0.09	0	0.01	-0.03	-0.02	0	0.06	0	0.05	0.05	0	-0.01	0	0.14	0.15	0.03	0.03	-3.44	-0.02	-0.02	-0.02	-0.01	-0.01
LCL	a	-0.09	0.4	-0.08	-0.06	0.04	0	0.59	-0.06	-0.64	-0.46	1	1.03	0	-2.18	-2.08	-0.41	-0.42	-0.41	-9.67	1.77	1.83	0.93	0.95
	m	-0.09	0.4	-0.08	-0.08	0.02	0	0.62	-0.07	-0.64	-0.46	1.01	1.04	0	-2.17	-2.07	-0.41	-0.42	-0.41	1.75	-9.63	1.85	0.94	0.95
	p	-0.09	0.42	-0.08	-0.12	-0.01	0	0.7	-0.1	-0.63	-0.45	1.05	1	0	-2.13	-2.02	-0.41	-0.42	-0.41	1.8	1.84	-9.56	0.97	0.99
ALL	a	-0.07	0.4	-0.05	1.52	1.09	0	1.01	-0.55	0.06	0.13	0.68	0.76	0	0.44	0.56	-0.19	-0.18	-0.16	0.73	0.75	0.77	-9.66	1.69
	p	-0.07	0.4	-0.05	1.58	1.13	0	1.01	-0.57	0.06	0.12	0.68	0.76	0	0.43	0.55	-0.19	-0.18	-0.16	0.72	0.74	0.76	1.64	-9.58

	Reference strains*																						
	Joint gaps [mm]		Strain [%]																				
	Lat	Med	aACL	pACL	aPCL	pPCL	OPL	mPC	m_mPC	l_mPC	IPC	a_dMCL	m_dMCL	p_dMCL	a_sMCL	m_sMCL	p_sMCL	aLCL	mLCL	pLCL	aALL	pALL
Initial epsr	21.89	16.37	14.83	19.63	0	11.3	10.4	14.93	9.41	19	15.01	0	5.99	5.67	3.96	3.75	3.44	13.5	13.55	13.91	14.66	14.55

Ligament	Bundle	Reference strains*																						
		epsr	Joint gaps [mm] (+/- difference from initial value)		Strain [%] (+/- difference from initial strain)																			
		+0.1	Lat	Med	aACL	pACL	aPCL	pPCL	OPL	mPC	m_mPC	l_mPC	IPC	a_dMCL	m_dMCL	p_dMCL	a_sMCL	m_sMCL	p_sMCL	aLCL	mLCL	pLCL	aALL	pALL
ACL	a	0.45	-0.05	-0.01	6.38	-1.53	0	0.67	0.03	0.2	0.31	0.17	-0.1	0	1.13	1.19	0.1	0.1	0.11	0.14	0.14	0.16	-0.51	-0.54
	p	0.45	-0.04	-0.02	-1.72	7.41	0	0.5	-0.03	0.16	0.26	0.14	-0.09	0	1.02	1.07	0.07	0.07	0.07	0.1	0.1	0.12	-0.4	-0.43
PCL	a	-0.36	-0.03	-0.02	0.4	0.31	4.8	-0.37	0.07	-0.16	-0.18	-0.13	-0.03	0	-0.62	-0.65	-0.07	-0.08	-0.08	-0.07	-0.08	-0.09	-0.02	-0.02
	p	0.07	-0.32	-0.25	1.99	1.64	0	7.67	1.04	-0.41	-1.64	-0.95	-0.19	0	-5.87	-5.67	-0.76	-0.82	-0.86	-0.04	-0.05	-0.09	-0.63	-0.64
OPL		0.2	0.38	-0.09	0.22	-0.24	0	3.19	7.71	0.76	0.62	0.99	0.45	0	3.2	3.68	0.11	0.15	0.23	0.47	0.51	0.59	1.71	1.8
PC**	m	0.17	-0.26	-0.36	2.45	2.02	0	-3.94	1.11	9.42	-2.13	-0.87	0.06	0	-5.99	-5.67	-1.07	-1.14	-1.18	0.46	0.46	0.43	-0.42	-0.42
	m_m	0.17	-0.16	-0.22	1.62	1.32	0	-2.48	0.61	0.2	8.65	-0.55	0.05	0	-5.17	-5.36	-0.71	-0.75	-0.77	0.29	0.29	0.27	-0.24	-0.24
	l_m	0.17	-0.15	-0.02	0.27	0.2	0	-0.67	0.16	-0.1	-0.14	10.68	-0.29	0	-0.35	-0.42	-0.02	-0.02	-0.03	-0.45	-0.46	-0.49	-0.32	-0.33
	l	0.17	-0.13	0.01	-0.19	-0.16	0	-0.26	0.07	0.09	0.06	-0.29	10.42	0	0.36	0.32	0.08	0.08	0.08	-0.43	-0.44	-0.45	-0.37	-0.37
dMCL	a	-0.07	-0.01	-0.02	0.18	0.15	0	-0.24	0.05	-0.18	-0.17	-0.04	0.03	4.94	-0.64	-0.66	-0.09	-0.09	-0.09	0.07	0.07	0.07	0	0
	m	0.4	-0.16	-0.24	1.87	1.54	0	-2.74	0.72	-0.12	-1.59	-0.57	0.1	0	4.89	-5.67	-0.77	-0.82	-0.84	0.4	0.4	0.38	-0.24	-0.24
	p	0.4	-0.16	-0.23	1.79	0	0	-2.67	0.72	-0.02	-1.52	-0.56	0.09	0	-5.55	4.86	-0.74	-0.79	-0.81	0.36	0.36	0.34	-0.25	-0.25
sMCL	a	0.11	0	-0.11	0.34	0.23	0	-0.56	0.04	-0.48	-0.44	-0.06	0.11	0	-1.47	-1.5	9.97	-0.31	-0.31	0.21	0.21	0.21	0.13	0.14
	m	0.11	0	-0.11	0.35	0.23	0	-0.59	0.06	-0.5	-0.45	-0.06	0.11	0	-1.51	-1.55	-0.3	9.93	-0.31	0.21	0.21	0.21	0.12	0.13
	p	0.11	-0.01	-0.11	0.34	0.23	0	-0.61	0.08	-0.49	-0.44	-0.08	0.09	0	-1.49	-1.53	-0.29	-0.31	9.9	0.19	0.19	0.19	0.1	0.11
LCL	a	0.11	-0.37	0.08	0.33	0.2	0	-0.69	0.11	0.58	0.41	-0.98	-0.96	0	2.09	1.97	0.42	0.43	0.42	9.44	-1.67	-1.74	-0.76	-0.77
	m	0.11	-0.37	0.08	0.35	0.22	0	-0.72	0.12	0.57	0.41	-0.99	-0.96	0	2.07	1.94	0.42	0.43	0.42	-1.64	9.39	-1.75	-0.77	-0.78
	p	0.11	-0.38	0.08	0.39	0.25	0	-0.78	0.15	0.57	0.4	-1.02	-0.98	0	2.06	1.93	0.42	0.43	0.42	-1.68	-1.72	9.31	-0.78	-0.79
ALL	a	0.13	-0.35	0.05	-1.31	-0.92	0	-0.88	0.57	0	-0.03	-0.56	-0.61	0	-0.18	-0.3	0.19	0.18	0.16	-0.6	-0.62	-0.64	9.62	-1.43
	p	0.13	-0.35	0.05	-1.36	-0.96	0	-0.87	0.59	0.01	-0.02	-0.55	-0.61	0	-0.16	-0.28	0.19	0.18	0.17	-0.59	-0.6	-0.63	-1.39	9.54

* Changed individually: if e.g. ACL_1 were changed, the rest of the ligament bundle settings were set to 'initial'
** PC is a capsule, but is modeled as 4 seperate ligament bundles in the TAKOM model

F. Tuning steps

The tuning steps in Table 3 were chosen based on the results of the sensitivity analysis as shown in Figure 6. During tuning, the thought process of each tuning step was written down. These explanations of each tuning step are described in Table F.1 below. Note that the medial and lateral gaps are the results of the valgus and varus laxity tests, respectively.

Table F.1: Tuning steps and their explanations, including the expected and actual changes in joint gaps

Tuning step	Expected change (w.r.t. previous tuning step)	Explanation	Actual resulting change (w.r.t. previous tuning step)
1	Medial gap +0.99 mm Lateral gap +0 mm	We want to increase the medial joint gap, but not too much to leave no space for tuning other ligaments if needed or to increase the strains in other ligaments too much	Medial gap +1.12 mm Lateral gap -0.34 mm
2	Medial gap +0.37 mm Lateral gap +0.04 mm	The strains in the dMCL bundles increased even more because of tuning step 1: this together with the fact that the medial gap needs to be larger led to this tuning step	Medial gap +0.3 mm Lateral gap +0.38 mm
3	Lateral gap +0.98 mm Medial gap -0.1 mm	The lateral side needs tuning as well: the LCL has the biggest effect here. Decreasing the reference strain with 0.1 is too much, but decreasing it with 0.05 is too little: we want something in between	Lateral gap +0.97 mm Medial gap -0.68 mm
4	Medial gap +0.53 mm Lateral gap +0.06 mm	To compensate for the effect of tuning the LCL on the medial gap, the medial side needs to be more lax. As the strains of the medial and middle-medial PC bundles increased the most, tuning these two PC bundles made the most sense	Medial gap +0.3 mm Lateral gap +0.29 mm
5	Medial gap -0.27 mm Lateral gap -0.21 mm	The lateral side is too lax now, so the tuning of the medial and middle-medial PC bundles should be partly reversed	Medial gap -0.15 mm Lateral gap -0.08 mm
6	Medial gap +0.5 mm Lateral gap +0 mm	The medial gap decreased after tuning step 5. Even though the strains of the sMCL bundles are not high, we can try to see what tuning the sMCL does, as the sensitivity analysis and tuning step 1 show that tuning the sMCL has a large effect on the medial gap	Medial gap +0.04 mm Lateral gap +0.01 mm
7	Medial gap +0.52 mm Lateral gap -0.73 mm	Tuning step 6 had little to no effect on both the medial and lateral side. Based on the strains, we could tune the dMCL again, but this will also increase the lateral gap, which we do not want now. Therefore, the next logical step based on the sensitivity analysis and the strains is to tune the OPL	Medial gap 0.49 mm Lateral gap -0.52 mm
8	Lateral gap +0.3 mm Medial gap -0.01 mm	To compensate for the decreased lateral gap after tuning step 7, the lateral side should be more lax. Based on the sensitivity analysis and the strains of the middle-lateral and lateral PC bundles, tuning these two PC bundles was a logical next step	Lateral gap +0.37 mm Medial gap -0.04 mm

9	Medial gap +0.055 mm Lateral gap +0.02 mm	Both the medial and lateral simulated joint gaps are now close to the measured joint gaps: the medial joint gap should be 0.12 mm larger and the lateral gap should be 0.06 mm larger. Therefore, we should tune a ligament bundle that results in an increased medial and lateral gap, where the effect on the medial gap should be around two times as large as on the lateral gap. Both bundles of the ACL seem to have an effect like this. As the strain of the anterior bundle of the ACL is much higher than that of the posterior bundle, we decrease the reference strain of the ACL bundle with 0.06	Medial gap +0.16 mm Lateral gap +0.05 mm

G. Tuning steps results

The effect of each tuning step on the joint gaps and ligament strains are shown below.

Valgus:

Increase or decrease w.r.t. initial values:

Green = decrease | Red = increase

0-25% | 26-50% | 51-75% | 76-100%

Initial gaps and strains	Laxity (joint gaps)		Strain																	
	Lat	Med	aACL	pACL	aPCL	pPCL	OPL	mPC	m_mPC	l_mPC	lPC	a_dMCL	m_dMCL	p_dMCL	a_sMCL	m_sMCL	p_sMCL	aLCL	mLCL	pLCL	aALL	pALL
	20.12	20.5	18.31	25.87	0	16.2	16	26.57	17.81	17.78	11.96	11.26	25.37	24.8	13.39	13.25	13.01	7.57	7.52	7.72	5.28	4.87

Tuning step	Adaptation	Laxity (joint gaps)		Strain																		
		Lat	Med	aACL	pACL	aPCL	pPCL	OPL	mPC	m_mPC	l_mPC	lPC	a_dMCL	m_dMCL	p_dMCL	a_sMCL	m_sMCL	p_sMCL	aLCL	mLCL	pLCL	aALL	pALL
1	sMCL all bundles epsr -0.1	19.8	21.62	20.93	28.94	0	19.97	16.4	30.72	20.77	18.2	11.63	17.65	32.82	32.44	4.94	4.88	4.72	15.84	6.29	6.48	4.02	3.57
2	dMCL all bundles epsr -0.05	19.49	21.92	19.02	28.02	0	22.13	17.1	32.34	22.11	19.25	12.13	11.46	28.56	28.31	6.19	6.14	6	7.47	7.44	7.7	2.98	2.46
3	LCL all bundles epsr -0.08	18.52	21.24	11.45	22.37	0	22.15	18.1	30.99	21.7	21.19	14.11	10.49	27.51	27.23	6.57	6.44	6.25	3.69	3.78	4.2	2.47	1.84
4	PC bundles 1&2 epsr -0.1	18.06	21.54	11.78	23.13	1.62	24.46	18.3	20.92	11.74	21.64	14.09	14.03	31.68	31.48	8.11	8	7.81	3.53	3.63	4.05	1.81	1.14
5	PC bundles 1&2 epsr +0.05	18.29	21.39	11.58	22.72	0.59	23.31	18.2	26.01	16.76	21.42	14.11	12.26	29.6	29.36	7.35	7.22	7.03	3.62	3.72	4.15	2.15	1.49
6	sMCL all bundles epsr -0.05	17.58	21.43	10.92	22.65	2.21	24.87	18.4	27.65	17.85	21.87	14.27	15.28	33.15	32.95	2.83	2.7	2.51	4.17	4.29	4.74	1.59	0.89
7	OPL epsr -0.1	16.8	21.92	9.59	22.05	1.75	23.43	10.7	28.09	19.08	22.5	15.22	17.85	36.1	35.79	3.92	3.79	3.62	5.15	5.33	5.85	0.3	0
8	PC bundles 3&4 epsr -0.1	16.64	21.88	8.94	21.57	2.43	23.58	10.9	28.23	20.01	11.42	4.83	18.28	36.58	36.26	4.1	3.96	3.79	5.82	6.02	6.57	0.54	0
9	ACL bundle 2 epsr -0.06	16.99	22.04	10.17	17.16	3.53	24.94	10.3	30.72	20.04	11.35	4.48	18.45	36.79	36.52	4.09	3.96	3.79	4.93	5.1	5.61	0.52	0

Varus:

Increase or decrease w.r.t. initial values:

Green = decrease | Red = increase

0-25% | 26-50% | 51-75% | 76-100%

Initial gaps and strains	Laxity (joint gaps)		Strain																	
	Lat	Med	aACL	pACL	aPCL	pPCL	OPL	mPC	m_mPC	l_mPC	lPC	a_dMCL	m_dMCL	p_dMCL	a_sMCL	m_sMCL	p_sMCL	aLCL	mLCL	pLCL	aALL	pALL
	21.89	16.37	14.83	19.63	0	11.3	10.4	14.93	9.41	19	15.01	0	5.99	5.67	3.96	3.75	3.44	13.5	13.55	13.91	14.66	14.55

Tuning step	Adaptation	Laxity (joint gaps)		Strain																		
		Lat	Med	aACL	pACL	aPCL	pPCL	OPL	mPC	m_mPC	l_mPC	lPC	a_dMCL	m_dMCL	p_dMCL	a_sMCL	m_sMCL	p_sMCL	aLCL	mLCL	pLCL	aALL	pALL
1	sMCL all bundles epsr -0.1	21.55	16.5	15.02	19.75	0	10.88	10.5	15.66	9.97	18.12	14.09	0	8.48	8.06	0	0	0	21.9	11.94	12.23	13.91	13.78
2	dMCL all bundles epsr -0.05	21.93	16.52	13.76	18.81	0	12.82	10.1	16.09	10.54	19.19	14.82	0	4.24	4.03	0	0	0	13.08	13.12	13.48	14.65	14.53
3	LCL all bundles epsr -0.08	22.9	16.19	15.06	20.11	0	12.46	10.4	13.25	8.17	21.5	17.71	0	0	0	0	0	0	8.66	8.78	9.26	17.2	17.13
4	PC bundles 1&2 epsr -0.1	23.19	16.52	13.33	18.75	0	16.51	10	5.07	0.6	22.47	17.85	0	3.9	3.97	0	0	0	8.21	8.33	8.82	17.7	17.63
5	PC bundles 1&2 epsr +0.05	23.08	16.41	13.88	19.15	0	15.08	10.1	9.48	4.74	22.13	17.77	0	0.45	0.47	0	0	0	8.36	8.48	8.97	17.47	17.39
6	sMCL all bundles epsr -0.05	23.09	16.42	13.84	19.11	0	15.2	10.1	9.56	4.81	22.15	17.77	0	0.7	0.73	0	0	0	8.34	8.47	8.96	17.48	17.41
7	OPL epsr -0.1	22.57	16.32	15.99	21.33	0	9.3	3.83	7.87	3.63	21.39	18.23	0	0	0	0	0	0	9.05	9.15	9.56	16.73	16.59
8	PC bundles 3&4 epsr -0.1	22.94	16.35	16.64	21.98	0	10.26	4.27	8.52	4.06	10.99	8.15	0	0	0	0	0	0	10.21	10.33	10.77	18.04	17.92
9	ACL bundle 2 epsr -0.06	22.99	16.34	17.98	17.59	0	9.81	4.46	8.11	3.93	10.96	8.29	0	0	0	0	0	0	10.28	10.39	10.82	18.44	18.33

Supplement 1: Measurement (intra-op. laxity tests) protocol *Subject no.* ☐

Surgery 1/2: CR-TKA

Done	Remarks/notes
Check exclusion criteria: - Severe lower-limb deformities - Limited range of motion (ROM) lower than 90° ☐ ☐	Remarks exclusion criteria:
I. Pre-operative data 1. Obtain pre-operative CT scan of the knee joint according to Mako Robotic System surgery protocol. 1. ☐	Where to find (e.g. file name):
2. Obtain pre-operative clinical record (if possible). 2. ☐	
II. Intra-operative measurements <u>before</u> bone resections 3. Are the following ligaments intact: • Posterior cruciate ligament (PCL) • Medial collateral ligament (MCL) • Lateral collateral ligament (LCL) Document the ligaments' condition evaluation. In case one or more ligaments are not intact, the measurements could be affected. 3. PCL ☐ MCL ☐ LCL ☐	Notes ligament condition:
4. Perform the following laxity measurements / tests, assessing the knee kinematics <u>at 0° and 90°</u>. *Note: this should be repeated twice!* **a. Anterior drawer test** Perform a laxity test with anterior stress (moving the tibia anteriorly). **b. Posterior drawer test** Perform a laxity test with posterior stress (moving the tibia posteriorly). **c. Varus stress test** Perform a laxity test with varus stress (moving the tibia medially: knee outward). **d. Valgus stress test** Perform a laxity test with valgus stress (moving the tibia laterally: knee inward). **e. Internal rotation test** Perform a laxity test with internal rotation stress (moving the toes inward). **f. External rotation test** Perform a laxity test with external rotation stress (moving the toes outward). During all the tests, record the 3D kinematics in terms of translations and rotations in order to determine the position of the femur.	4. Test (2x) 3D kin. (2x) a. T1 T2 T1 T2 0° ☐☐ ☐☐ 90° ☐☐ ☐☐ b. T1 T2 T1 T2 0° ☐☐ ☐☐ 90° ☐☐ ☐☐ c. T1 T2 T1 T2 0° ☐☐ ☐☐ 90° ☐☐ ☐☐ d. T1 T2 T1 T2 0° ☐☐ ☐☐ 90° ☐☐ ☐☐ e. T1 T2 T1 T2 0° ☐☐ ☐☐ 90° ☐☐ ☐☐ f. T1 T2 T1 T2 0° ☐☐ ☐☐ 90° ☐☐ ☐☐	*Take photos of the screen!!!* *or* *See tables of test rounds for measurement values* Other remarks: Where to find (e.g. file name):

	Done	Remarks/notes
5. Record the tibiofemoral joint kinematics: move the knee from full extension to maximally achievable knee flexion, and record the 3D kinematics in terms of translations and rotations in order to determine the position of the femur and tibia during the movement. *Note: this should be repeated 3 times!*	5. Rep. 1 ☐ Rep. 2 ☐ Rep. 3 ☐	Where to find (e.g. file name):
III. Intra-operative bone resection and placement of the implant 6. Perform the bone resection and implant placement according to the guidelines used at Policlinico di Modena.	6. ☐	Remarks implant placement:
IIII. Intra-operative measurements <u>after</u> bone resections and placement of the implant 7. Repeat step 4: Perform a post-implant assessment of the laxity of the ligaments (still intra-operative) by performing step 4 again (twice for 0° as well as 90°). **a. Anterior drawer test** Perform a laxity test with anterior stress (moving the tibia anteriorly). **b. Posterior drawer test** Perform a laxity test with posterior stress (moving the tibia posteriorly). **c. Varus stress test** Perform a laxity test with varus stress (moving the tibia medially: knee outward). **d. Valgus stress test** Perform a laxity test with valgus stress (moving the tibia laterally: knee inward). **e. Internal rotation test** Perform a laxity test with internal rotation stress (moving the toes inward). **f. External rotation test** Perform a laxity test with external rotation stress (moving the toes outward). During all the tests, record the 3D kinematics in terms of translations and rotations in order to determine the position of the femur.	7. Test (2x) / 3D kin. (2x) a. T1 T2 / T1 T2 0° ☐☐ ☐☐ 90° ☐☐ ☐☐ b. T1 T2 / T1 T2 0° ☐☐ ☐☐ 90° ☐☐ ☐☐ c. T1 T2 / T1 T2 0° ☐☐ ☐☐ 90° ☐☐ ☐☐ d. T1 T2 / T1 T2 0° ☐☐ ☐☐ 90° ☐☐ ☐☐ e. T1 T2 / T1 T2 0° ☐☐ ☐☐ 90° ☐☐ ☐☐ f. T1 T2 / T1 T2 0° ☐☐ ☐☐ 90° ☐☐ ☐☐	*Take photos of the screen!!!* *or* *See tables of test rounds for measurement values* Other remarks: Where to find (e.g. file name):
8. Repeat step 5: Record the tibiofemoral joint kinematics: move the knee from full extension to maximally achievable knee flexion, and record the 3D kinematics in terms of translations and rotations in order to determine the position of the femur and tibia during the movement.	8. Rep. 1 ☐ Rep. 2 ☐ Rep. 3 ☐	Where to find (e.g. file name):

Supplement 2: Workflow for TKA including Laxity Measurements

Flow diagram TKA and measurement workflow

The steps in the flow diagram below will be explained in the next section of this document. The flow diagram is only meant to visualize the workflow. The arrows on the left indicat the normal surgical workflow, the arrows on the right indicate the workflow with the laxity measurements added.

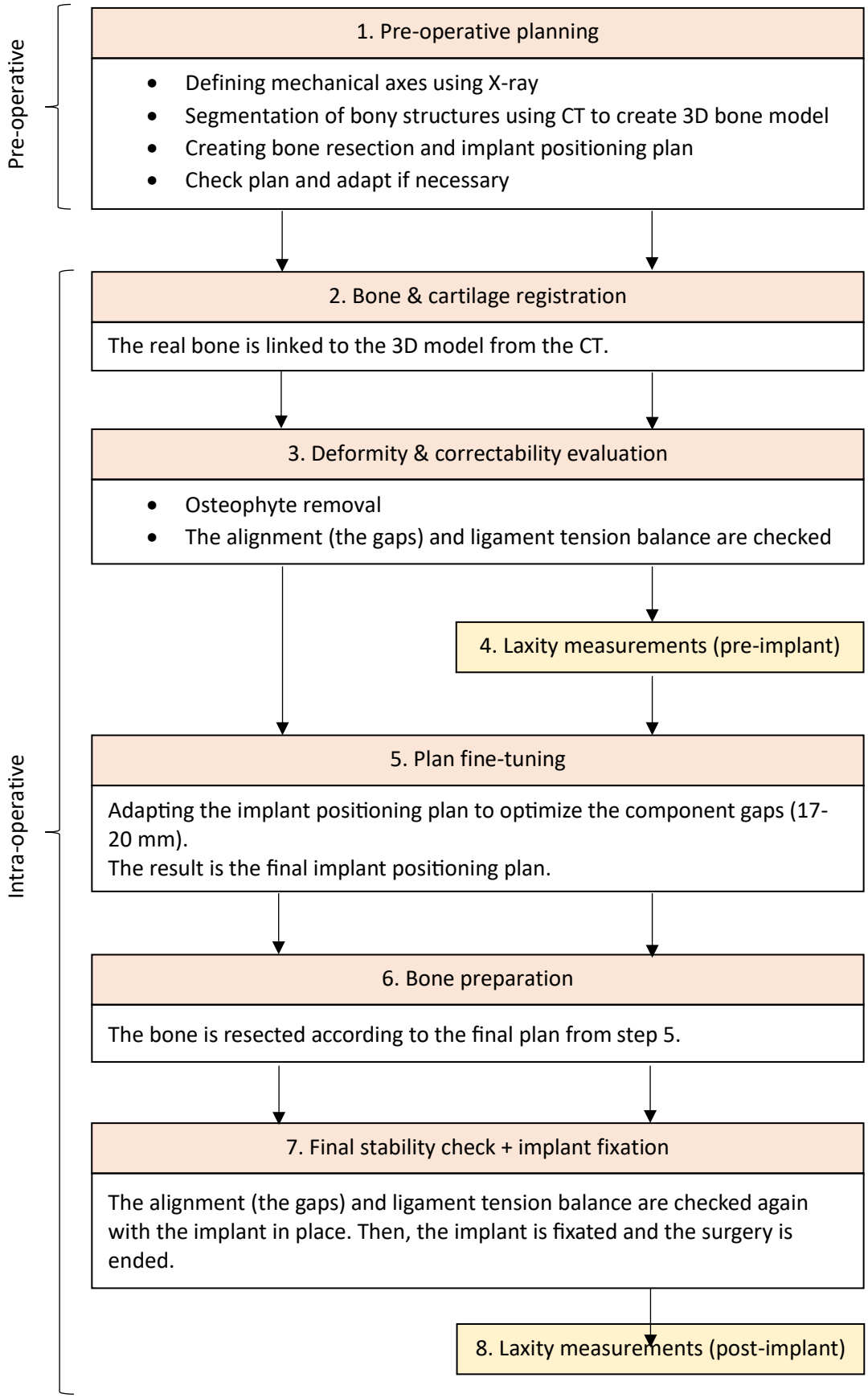

Explanation TKA and measurement workflow

The entire TKA workflow can be described by steps. The following steps also include the laxity measurement tests performed in Modena, which are shown in cursive. Step 2-8 are all intra-operative. [S1]

1. Preoperative planning
2. Bone and cartilage registration
3. Deformity and correctability evaluation
4. *Laxity measurements (pre-implant)*
5. Plan fine-tuning
6. Bone preperation
7. Final joint stability check + implant fixation
8. *Laxity measurements (post-implant)*

For this workflow, the measurement data from research subject 4 was used.

1. Preoperative planning

The first step is to observe the patient's anatomy and define the femoral and tibial mechanical axis and different angles based on those axes using an X-ray of the legs. The five angles that are determined are the Mechanical Lateral Distal Femoral Angle (mLDFA), the Mechanical Medial Proximal Tibial Angle (mMPTA), the Joint Line Convergence Angle (JLCA), the Tibial Posterior Slope (tPS, not shown in figure) and the mechanical Femoro-Tibial Angle (mFTA), see Figure S2.1.

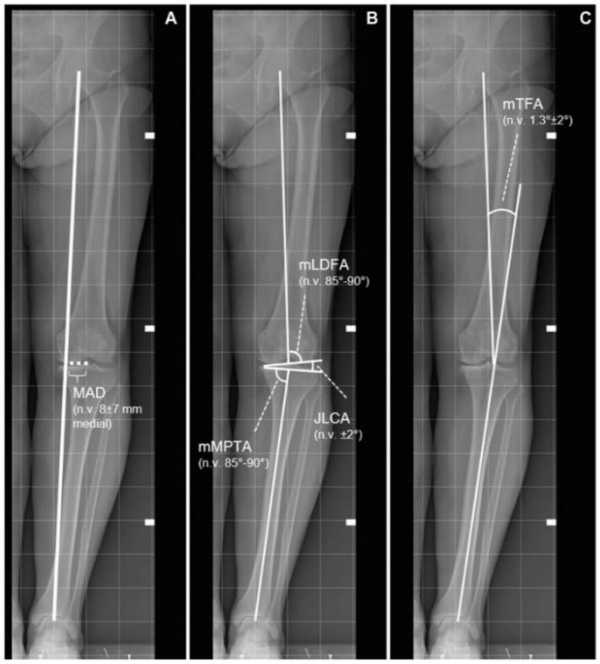

Figure S2.1 Preoperative X-ray with mechanical axes and angles [1]

The femoral and tibial mechanical axis are also used by the robotic surgery system and thus also for the CT-based preoperative planning. For the CT based planning, a CT scan of the knee, hip and ankle is used to define the femoral and tibial mechanical axis in 3D by using bony landmarks, defined by the MAKO specialist. The CT scan is also segmented. The segmented CT is used to automatically generate resection landmarks. The resection landmarks are used to compute the medial and lateral resection thickness of the distal femur, posterior femur and proximal tibia. The resection landmarks can be adjusted manually, for example when they are located on an osteophyte. Also, the implant positioning is determined. [S2]

An example of a preoperative plan based on the CT is shown in Figure S2.2 (research subject 4 (TKA subject 3)). The pre-operative plan shows the planned implant positioning made by the MAKO specialist.

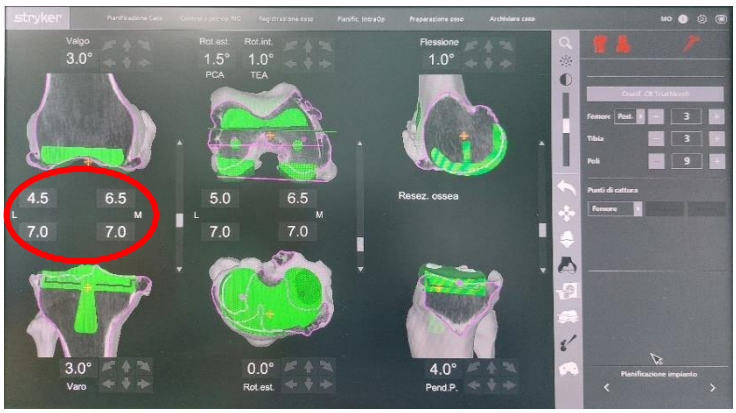

Figure S2.2 Preoperative CT-based implant positioning and bone resection plan

The values highlighted by the red circle are the medial and lateral bone resection depths (the cartilage is already accounted for in the planning). The medial side has a smaller resection depth, generally because this side is more affected (more bone wear). The values at the top and the bottom are the varus/valgus angle, internal and external rotation, flexion angle, and posterior tibial slope of the implant with respect to the mechanical axes.

The values on the right of the screen are the sizes of the femoral and tibial implant component. These sizes do however not affect the thickness of the implant components; these are always 8.5 mm and 9 mm for the femoral and tibial component, respectively. This is the reason why the desired joint gap is 17-18 mm (8.5 + 9 = 17.5 mm) [S1][S3].

Right before surgery, the surgeon checks the plan the MAKO specialist created and makes adjustments if considered necessary. He will do this by checking the planned position of the implant, but also the implant component size, to avoid femoral notching (which could increase stresses and cause femoral fractures), overhang of the components, and incomplete resections. [S1]
When performing preoperative planning of the implant positioning, implant planning guidelines in terms of rotational allignment, resection depth, and component size are followed. [S2]

2. Bone and cartilage registration

Bone arrays with optical markers are attached to the femur and the tibia, and the visibility of the arrays on the system camera throughout the full ROM is verified.

The surgeon then performs bone registration by touching bony landmarks with a probe (which also has optical markers attached) to link the bone to the 3D bone model determined from the CT scan.

After bone registration, the cartilage thickness can be assessed by touching different parts of the femur and tibia with the probe. This way, the distance between the bony surface and the tip of the probe and thus the thickness of the cartilage can be determined. This step is not strictly necessary, because the planning is based on bony resections, as explained before. [S1]

3. Deformity and correctability evaluation

Osteophytes that are in the way of and creating tension in surrounding soft tissue structures, are removed. With the initial plan, deformity and correctability evaluation is performed by looking at the joint gaps in real time (see Figure S2.3). On the same screen, the angles of the implants with respect to the mechanical axes can be seen again, as well as the real time flexion and varus/valgus angle of the knee (highlighted with the green circle). This is also the point in surgery where the pre-implant laxity measurements were done, which will be explained in the next paragraph.

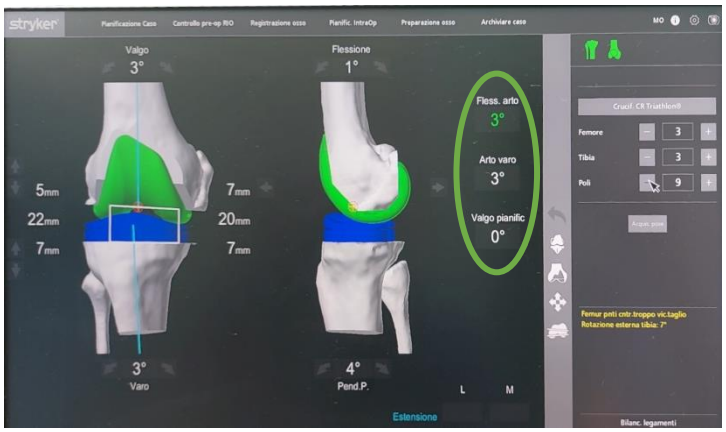

Figure S2.3 MAKO screen showing real time component gaps and angles

For the deformity and correctability evaluation, the ligaments are tensioned with spacer spoons, because the joint gaps are defined as the gaps between the osteotomies (the resected bone). If not tensioned, the gap would not fit an implant of 17.5 mm in total. By applying the tension, the surgeon can see on the MAKO screen (see Figure S2.3 for an example of research subject 4 (TKA subject 3)) if the collateral ligament tension is balanced and what the compartment gaps and alignment would look like after bone resection with the initial implant positioning plan. This is done both in flexion and extension. [S1]

In extension, the surgeon will use the spoon to create tension on the least affected side and apply an opposite stress. It is important to note that the tension created with the spacer spoons and the varus/valgus stress applied are not the same thing. In this case, the patient has a varus knee. So, the surgeon places a spoon on the lateral side, to apply tension to the ligaments on that side. Then, he applies a valgus stress to open up the affected side (the medial side in this case). This way, he can see the joint gaps based on the pre-operative plan. With this information, the pre-operative plan can be adjusted in order to get to the desired gaps (this will be explained later).
In flexion, spoons are placed on both the lateral and medial side, so tension is applied simultaniously on both sides.

4. Laxity measurements (pre-implant)

During the deformity evaluation, the pre-implant laxity measurements were done, as they overlap with the evaluation step. The evaluation step only contains a valgus stress test for a varus knee (or a varus stress test if the patient has a valgus knee). For the laxity measurements, a no stress situation and a varus stress test (or valgus stress test) are added, for both extension and 90° flexion. This means that for both extension and 90° flexion, we have a flexion angle, varus angle, and lateral and medial joint gap for 3 situations: no stress, varus stress and valgus stress. Note that 'no stress' does not mean 'no tension': there is still tension applied by the spacer spoon, there is just no varus or valgus stress applied. The values obtained from the MAKO screen (which was displayed as in Figure 3), can be seen in Table S2.1.

Table S2.1 Pre-implant laxity measurement results for research subject 4

Pre-implant				
No stress	Actual angle (deg)	Varus (deg)	Joint gap lat. (mm)	Joint gap med. (mm)
0 deg	3	3	22	20
90 deg	90	1	18	18
Varus stress	Actual angle (deg)	Varus (deg)	Joint gap lat. (mm)	Joint gap med. (mm)
0 deg	4	9	23	17
90 deg	89	3	20	x*
Valgus stress	Actual angle (deg)	Varus (deg)	Joint gap lat. (mm)	Joint gap med. (mm)
0 deg	2	2	21	22
90 deg	89	3	x*	19

*These cannot be measured, as for 90 degrees knee flexion, we cannot do valgus stress and varus stress seperately: the surgeon places a spoon below the femur on both the lateral and medial side and then applies stress, so the gap opens up simultaneously medial and lateral. In this case, the laxity is |18-20| = 2 mm laterally and |18-19| = 1 mm medially.

Table S2.1 shows that in the no stress situation, the varus angle for 'full extension' (the actual flexion angle was 3°) is 3° and the component gaps are 22 mm and 20 mm for the lateral and medial side, respectively.
When applying varus stress, the varus angle, of course, becomes bigger (9°). The lateral gap increases and becomes 23 mm, and the medial gap decreases and becomes 17 mm. The valgus stress results can be read in the same way. Therefore, the difference (delta), and thus the laxity between the no stress and varus/valgus stress situations is thus 23 – 22 = 1 mm laterally and 22 – 20 = 2 mm medially. To make it more clear, the values used for determining this laxity are circled in Table S2.1. The 90° flexion tests can be read in the same way as the extension tests.

5. Plan fine-tuning

The goal is to have a medial and lateral gap that are almost the same in both flexion and extension. The size of these gaps slightly differ in literature, but when taking the average advised component gap in research by Andrea Ensini et al. [S1] and Zambianchi et al. [S3] and a meeting with Dr. Zambianchi, a gap of 17-18 is advised, where the lateral gap can be slightly bigger (preferably 1 mm) than the medial gap.
The gap measurements of paragraph 3 are used to adapt the initial implant position and bone resection plan: the plan (so the size, rotation angles and/or postioning) is changed so that the component gaps become 17-18 mm as mentioned before. This is done at the same time, so while creating the ligament tension (paragraph 3), the implant positioning is adapted. An example of the needed fine-tuning steps can be seen in Figure S2.4.

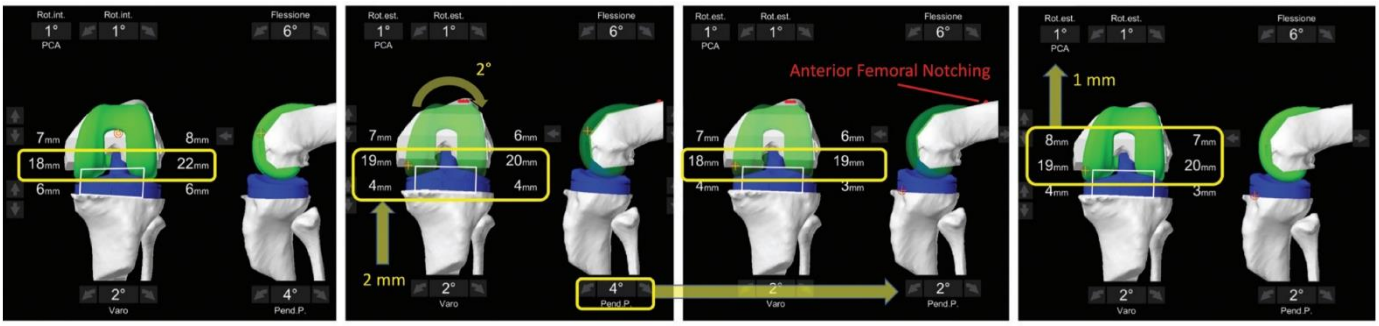

Figure S2.4 Intra-operative fine-tuning steps to adjust the component gap in flexion [1]

The final implant positioning and bone resection plan can then be displayed in the same way as Figure S2.2, showing the new values. For subject 4 (TKA subject 3), the final plan is shown in Figure S2.5.

As shown in Table S2.1, the joint gaps based on the initial plan were too large (20 or higher). In order to achieve joint gaps of 17-18, less bone should be resected. Therefore, the resection depths of 4.5 mm, 7 mm, 6.5 mm and 7 mm as shown in Figure 2, were changed to 2.5 mm, 6 mm, 5 mm and 6 mm as shown in Figure S2.5.
The implant component angles were left the way they were initially planned.

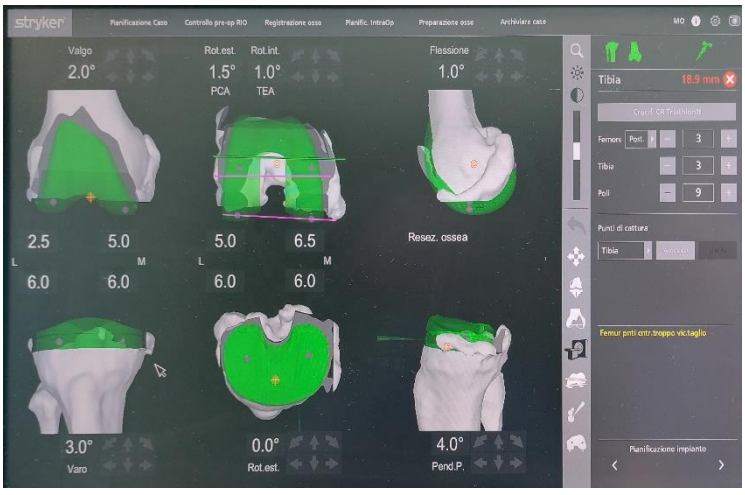

Figure S2.5 Final plan of implant positioning and bone resection

6. Bone preparation

Based on the implant positioning and bone resection planning, the MAKO system creates a 3D plan of the resection sites / cutting planes.

The saw also has optical markers, so the surgeon can see what he is doing in real time on the MAKO screen, see Figure S2.6. The screen shows in green what parts of the bone should be resected. Correctly resected bone turns white during resection. During resection, the robot gives haptic feedback to prevent the surgeon from resection too much bone: if the saw moves 0.5 mm deeper than the planned resection, an audio warning is given by the system. If the saw moves 0.75 mm deeper than the planned resection, the saw will automatically be disabled and the over-resected bone will appear red on the MAKO screen. [S2]

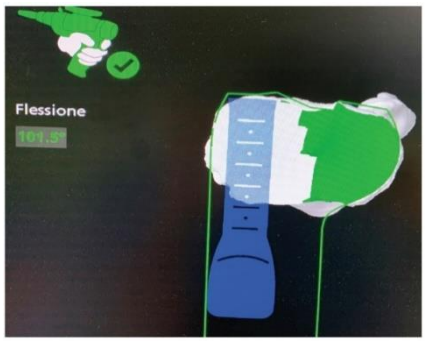

Figure S2.6 Resection mode of the MAKO system [1]

7. Final joint stability check + implant fixation

The final step of the surgery is to check the final stability and component gaps with trial components (so the components are not fixated yet, but just placed onto the resected bones in order to perform this step). The surgeon will place the leg in extension and flexion again, like in paragraph 3, to assess the component gaps and he will apply stress again to assess the ligament stability. The values for this assessment will be displayed in the same way as Figure S2.3. After this assessment, the components are fixated and the surgery is ended.

8. Laxity measurements (post-implant)

These are the post-implant measurements as described in the protocol, performed after the implant components are fixated. Again, for both extension and 90° flexion, the component gaps and the angles (varus and flexion) were measured for 3 situations: applying no stress, applying varus stress and applying valgus stress. These measurements are based on the final implant positioning plan, which were shown in Figure S2.5 above.

Table S2.2 Post-implant laxity measurement results for research subject 4

Post-implant				
No stress	Actual angle (deg)	Varus (deg)	Joint gap lat. (mm)	Joint gap med. (mm)
0 deg	0	1	19	18
90 deg	92	3	20	20
Varus stress	Actual angle (deg)	Varus (deg)	Joint gap lat. (mm)	Joint gap med. (mm)
0 deg	0	4	20	18
90 deg	92	2	20	20
Valgus stress	Actual angle (deg)	Varus (deg)	Joint gap lat. (mm)	Joint gap med. (mm)
0 deg	1	0	18	19
90 deg	93	2	20	20

Table S2.2 shows that in the no stress situation, the varus angle for full extension has been brought back from 3° to 1° and the joint gap is now more equal for the lateral and medial side and closer to the desired joint gap of 17-18 mm (19 and 18 mm as opposed to 22 and 20 mm).
When applying varus stress, the varus angle again becomes bigger (4°) and the lateral gap increases from 19 to 20 mm and the medial gap decreases from 18 to 19 mm. Thus, the laxity post-implant is 20 – 19 = 1 mm laterally and 19 – 18 = 1 mm. The values used for determining this laxity are circled in Table S2.2. The valgus stress results can be read in the same way again.

For this subject, the laxity itself did not change much (it was already low to begin with), but the joint gaps and the varus angle were improved.

Also, we can see that this subject had only a mild varus deformity (3° in extension and improved to 1°). For patients with a bigger deformity, the varus/valgus is usually not brought back too close to 0°, in order to match the other leg and thus to retain a natural gate, but also because research shows that a neutral alignment is not the optimal alignment for patients with a natural varus. Research by Bellemans et al. [S4] showed that a big fraction of the normal population has a natural alignment of 3° varus or more. Therefore, restoring of mechanical alignment to 0° varus would be unnatural for these patients. Furthermore, a follow-up study by Vanlommel [S5] showed that patients with pre-operative varus had better clinical and functional outcome scores if the post-operative alignment was in mild varus, compared to patients with a post-operative neutral (0° varus) alignment.

References

[S1] A. Ensini, F. Zambianchi, A. Illuminati, and F. Catani, “Isolated patellofemoral (PFJ) and biunicompartmental (BIUKA) makoplasty,” in *Robotic surgery for total hip and knee replacement*, 2019.

[S2] Stryker, “MAKO TKA Surgical Guide.” [Online]. Available: https://www.strykermeded.com/media/2223/mako-tka-surgical-guide.pdf.

[S3] F. Zambianchi *et al.*, “Joint line is restored in robotic-arm-assisted total knee arthroplasty performed with a tibia-based functional alignment,” *Arch. Orthop. Trauma Surg.*, vol. 141, no. 12, pp. 2175–2184, Dec. 2021, doi: 10.1007/S00402-021-04039-Z.

[S4] J. Bellemans, W. Colyn, H. Vandenneucker, and J. Victor, “The Chitranjan Ranawat Award Is Neutral Mechanical Alignment Normal for All Patients? The Concept of Constitutional Varus,” doi: 10.1007/s11999-011-1936-5.

[S5] L. Vanlommel, J. Vanlommel, S. Claes, and J. Bellemans, “Slight undercorrection following total knee arthroplasty results in superior clinical outcomes in varus knees,” *Knee Surgery, Sport. Traumatol. Arthrosc.*, vol. 21, no. 10, pp. 2325–2330, Oct. 2013, doi: 10.1007/S00167-013-2481-4.

Supplement 3: CT postprocessing workflow

In order to use the CT data in AnyBody, it first has to be postprocessed in ImageExplorer. There are several steps that need to be done:

1. Segmentation
2. Postprocessing of the segmentation
3. Cartilage estimation
4. Landmark definition
5. Putting the CT data into AnyBody

These steps are further explained below.

1. Segmentation

To extract the bony structures from the CT scans, segmentation has to be done, for which existing segmentation models are used. There are four available segmentation models: two for the knee (which I will use for segmentation), one for the hip, and one for the ankle. The two models for the knee are:

- Model 47: This model is purely used for visualizing the bones (surface mesh) and for the contact surfaces. When running this segmentation model, the output will consist of separate segmentations of
    - the distal femur
    - the proximal tibia
    - the patella

  of both the 'refined' bony structures (includes the osteophytes) and the 'premorbid' bony structures (an estimation of the healthy bones). This premorbid segmentation will be used for the laxity tests in AnyBody, because the laxity tests in Modena were done after removal of the osteophytes. The segmentation of Model 47 can be seen in Figure S3.1A.
- Model 65: This model gives the same output as Model 47, but with lower quality, which can clearly be seen in Figure S3.1B. This segmentation is used for the definition of the landmarks, as the unrefined part of the segmentation contains corresponding vertices and landmarks. This means that the indices of the vertices where the landmarks are defined, will always be the same.

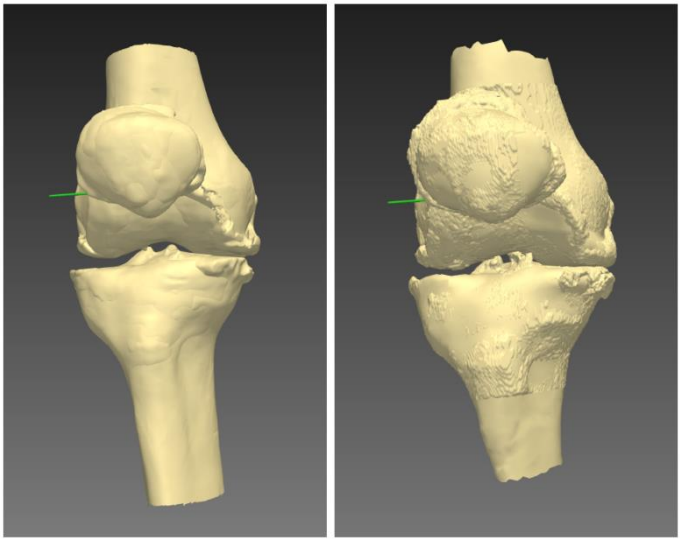

Figure S3.1 A) Segmentation using Model 47 and B) Segmentation using Model 65 for subject 4

2. Postprocessing of the segmentation

The resulting segmentation from the models is good, but can be improved by doing some postprocessing steps:

- Plane intersection: with this tool, the region of interest can be made smaller, for example for the tibia (we only need the proximal tibia, so the part of the tibia we do not need can be removed).
- Closing holes: this step is not really necessary, but with this tool, the holes in the mesh where the region of interest cut off the femur and tibia during segmentation can be closed. When doing the plane intersection step, this step is done automatically.
- Remeshing: the segmentation will create a mesh that does not yet consist of equal triangles. This can be fixed by applying remeshing. By remeshing, the bone surface will be more accurate.
- Smoothing: with this tool, the mesh will be smoothed, mainly for wrapping of the soft tissues around the bones. In this step, Laplacian smoothing is used (each vertex will get a new position based local factors). The number of iterations will define how much the mesh is smoothed. As we want a smooth enough surface for the ligaments and muscles to wrap around, but we do not want to lose too much information on the bones, an iteration number of 1 (max. 2) should be applied. This way, all 'sharp' edges will be removed, but the bones will keep their structure.

These steps should be done for the Model 47 segmentation (premorbid version) as well as the Model 65 segmentation (unrefined version).

3. Cartilage estimation

In order to account for the thickness of the cartilage (for the contact forces as well as determining the joint gaps), the cartilage has to be estimated based on the bony structures in the CT scans. For this, another existing model is used in ImageExplorer.
The output is another surface mesh that includes the estimated cartilage.

4. Landmark definition

For scaling purposes, different landmarks should be defined on the surface mesh. Some landmarks are already defined by Stryker, but additional landmarks can be extracted from the resulting .pts-file from step 1 (model 65). The following list contains all the landmarks, including the ones provided by Stryker:

- Landmark of the hip: hip center
- Landmarks of the femur: lateral epicondyle, medial epicondyle, trochlear center, distal medial resection, distal lateral resection, posterior medial resection, posterior lateral resection, and anterior proximal
- Landmarks of the tibia: tibial knee center, tibial medial resection, tibial lateral resection, anterior rotational, posterior rotational, tibial tuberosity, medial peak, lateral peak, Gerdys tubercle, medial tuberosity, lateral tuberosity, medial intercondylar tubercle, lateral intercondylar tubercle, distal anterior, medial tibial condyle, and lateral tibial condyle
- Landmarks of the patella: lateral patellar border, medial patellar border, patellar base, and patellar apex
- Landmarks of the ankle: medial malleolus and lateral malleolus

5. Putting the CT data into AnyBody

The resulting landmark coordinates should be pasted into the following AnyBody files:

- The coordinates in ‘points1’ (target points) in:
    - \Application\Subjects\R015\Osteophytes-free\Transformation\FemurTransformation.any
    - \Application\Subjects\R015\Osteophytes-free\Transformation\TibiaTransformation.any
    - \Application\Subjects\R015\Osteophytes-free\Transformation\PatellaTransformation.any
- The coordinates in \Application\Model\S04\Osteophytes-free\ModelParameters.any

The resulting STL files should be put into the ‘reconstructed’ and ‘wrapping folders’ in the folder \Application\Subjects\R015\Osteophytes-free\Knee STLs. Furthermore, the STL file paths should be pasted into \Application\Model\S04\Osteophytes-free\ModelParameters.any for the contact and wrapping surfaces, and in \FDK\C926-to-TLEM-template\ModelParameters.any.